FORMATION AND DRAINAGE OF GLACIER DAMMED DAŃ ZHÙR (DONJEK) LAKE, YUKON

MOYA PAINTER

Thesis submitted to the University of Ottawa
in partial Fulfillment of the requirements for the
M.Sc. in Physical Geography

Department of Geography, Environment and Geomatics
Faculty of Arts
University of Ottawa

Table of Contents

List of Tables

List of Figures

Abstract

Dań Zhùr (Donjek) Glacier, located in the St. Elias Mountains, Yukon, is a surge-type glacier that undergoes cyclical periods of rapid advance over a period of ~1-2 years, followed by retreat for a period of ~10 years (Kochtitzky et al., 2019). Dań Zhùr Chù' (Donjek River) runs perpendicular to the terminus of the glacier and past surges have, at times, caused the terminus to advance enough to block the river, leading to the formation of an ice-dammed lake (Kochtitzky et al., 2020). The glacier most recently surged between 2012 and 2014, and since then Dań Zhùr Lake has drained three times: in 2017, 2018 and 2019. When a glacier dam fails, the drainage of the lake can be catastrophic and cause flooding downstream. In the case of Dań Zhùr Lake, the most recent drainage event occurred on July 13th, 2019, when the ~2.45 km^2 lake drained in less than 36 hours and created an ice canyon through the glacier terminus. Time-lapse cameras and pressure sensors were used to capture the drainage event, and air photos taken during the melt season (June and September) were used to construct digital elevation models (DEMs) of the glacier terminus, lake, and lake basin.

The method of drainage for the 2019 event was determined to be flotation of the terminus, leading to rapid subglacial drainage of the lake. There were also noticeable changes in water extent downstream during the 2019 event, meaning that there is a potential risk to downstream recreational users. Because of the formation of a large ice canyon after the 2019 drainage, it is very unlikely that that the lake will reform until the next surge, which is anticipated to occur around 2024. Following that surge, the size of Dań Zhùr Lake is expected to increase during the next quiescent phase, as the continued glacier recession will expose a larger basin for the lake to form in, and flotation will continue to be a likely mechanism for drainage. However, in the long term it is unlikely that ice-dammed lakes will continue to form at Dań Zhùr Glacier, as there is a trend of the maximum terminus extent during each surge being smaller than the previous one, meaning that the glacier will no longer block the flow of Dań Zhùr Chù'.

Acknowledgements

I would like to begin by acknowledging that the research throughout this project was conducted on Kluane First Nation Traditional Territory, and I would like to thank the community as a whole for being supportive throughout this process and allowing this research to take place. I would specifically like to recognize Kate Ballegooyen and Rachael Thom at Kluane First Nation for taking the time to communicate with me. I would also like to thank Carmen Wong at Parks Canada for her interest and support throughout this project.

Support for this research has been provided by the University of Ottawa, University of Waterloo, the Northern Scientific Training Program, the W. Garfield Weston Foundation, the Association of Canadian Universities for Northern Studies, the Yukon Government, the Yukon Foundation Scholarships, the Remote-Ex Norwegian/Canadian/American Partnership Program, the Natural Sciences and Engineering Research Council of Canada, Planet Labs Education and Research Program, the Polar Continental Shelf Program, and Kluane Lake Research Station.

I would like to express my sincere appreciation to both my supervisors Dr. Luke Copland (University of Ottawa) and Dr. Christine Dow (University of Waterloo) for being two of the most amazing and supportive supervisors I could have asked for. To Luke, you have been an amazing mentor throughout this whole process, always giving up your time to answer any question or concern, at any time. To Christine, thank you for being a voice of reason in so many circumstances, and for providing me and many other with an amazing example of a strong female scientist. Thank you both for providing me with opportunities I never dreamed of, from attending conferences in the Alps, to studying abroad in Svalbard. These are memories I will cherish forever. I would also like to acknowledge my thesis committee: Dr. Anders Knudby and Dr. Antoni Lewkowicz for providing helpful feedback and support throughout this process.

I would like to thank all the members of the Laboratory for Cryospheric Research over the past two years, as well as other members of the University of Ottawa Department of Geography, Environment and Geomatics. Thank you all for the advice, words of encouragement and never-failing fun times. I wish we all could have spent more time together in person. Finally, I would like to thank my family and close friends for their unwavering support. I am so grateful for the encouragement throughout this process.

1.0 Introduction

Dań Zhùr (Donjek) Glacier, located in the St. Elias Mountains, Yukon, is a surge-type glacier that undergoes cyclical periods of rapid advance over a period of ~1-2 years, followed by retreat for a period of ~10 years (Kochtitzky et al., 2019). Dań Zhùr Chù' (Donjek River) runs parallel to the terminus of the glacier and past surges have, at times, caused the terminus to advance enough to block the river, leading to the formation of an ice-dammed lake (Kochtitzky et al., 2020). The glacier most recently surged between 2012 and 2014, and since then Dań Zhùr Lake has drained three times: in 2017, 2018 and 2019. When a glacier dam fails, the drainage of the lake can be catastrophic and cause flooding downstream. In the case of Dań Zhùr Lake, the most recent drainage event occurred on July 13th, 2019, when the ~2.45 km^2 lake drained in less than 36 hours and created an ice canyon through the glacier terminus. Time-lapse cameras and pressure sensors were used to capture the drainage event, and air photos taken in July and September were used to construct digital elevation models (DEMs) of the glacier terminus, lake, and lake basin. In this study, satellite imagery, air photos, time-lapse cameras, DEMs and pressure transducer data are used to provide detailed information on Dań Zhùr Lake formation, drainage patterns, and downstream risks over the past few decades.

1.1 Study Area

Dań Zhùr Lake forms at the terminus of Dań Zhùr Glacier (61°11′14″ N, 139°31′30″ W), which is situated in the St. Elias Mountains, Southwest Yukon. The Dań Zhùr region forms part of Kluane First Nation traditional territory and is located within Kluane National Park and Reserve (Figure 1.1). This area of the Yukon is largely unpopulated and undeveloped, and the largest infrastructure in the area is the Dań Zhùr Chù' Bridge on the Alaska Highway, about 50 km downstream of Dań Zhùr Glacier. The highway is used as the main access road from the Yukon to Alaska and is a popular route for tourists and locals, especially during the summer months. A possible risk associated with the drainage of Dań Zhùr Lake is flooding in downstream areas between the glacier terminus and the area where the Alaska Highway bridge crosses the Dań Zhùr Chù'.

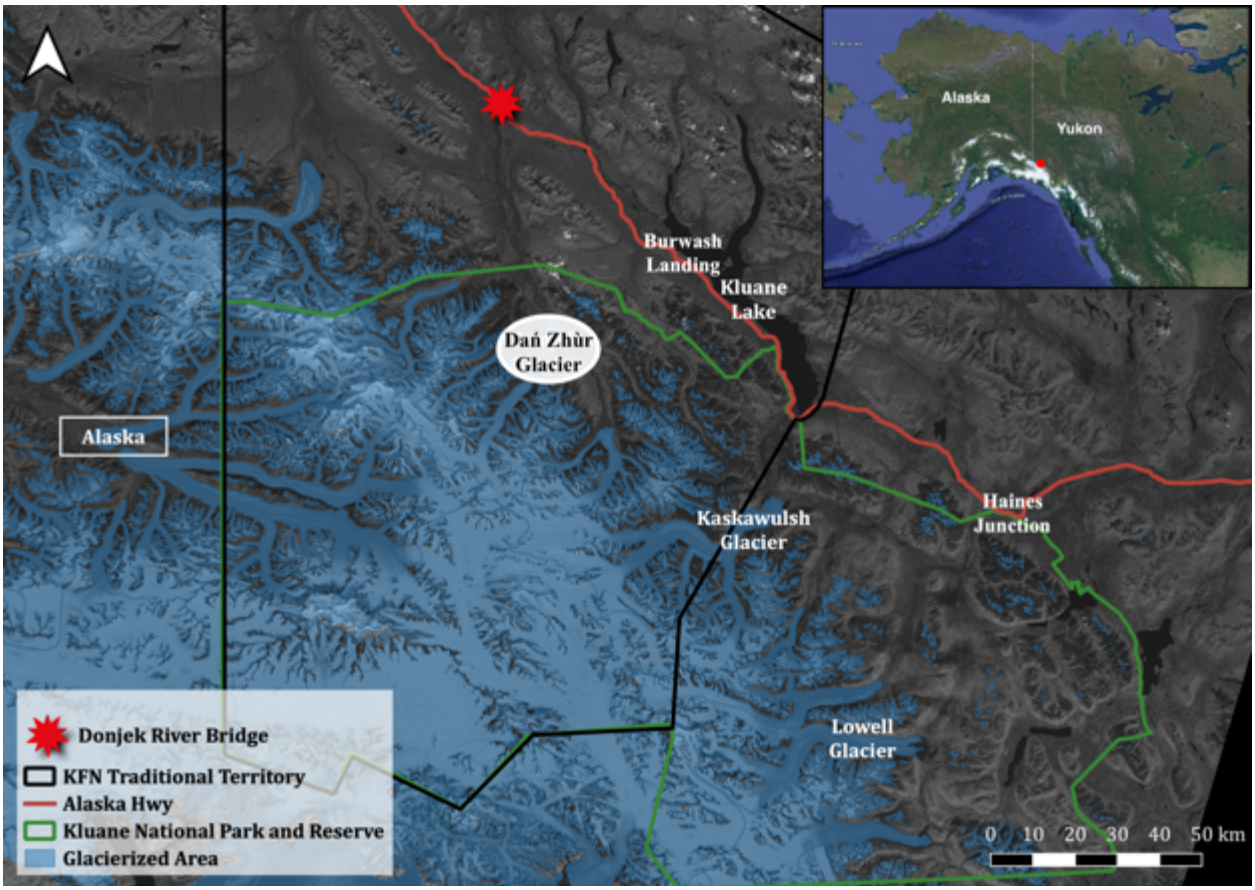

Figure 1.1. Location of Dań Zhùr Glacier within Kluane National Park and KFN Traditional Territory.

Dań Zhùr Glacier has surged approximately every 12 years since at least the 1930s (Kochtitzky et al., 2019). There have been eight surge events of Dań Zhùr Glacier since 1935: in ~1935, ~1947, late-1950s, ~1969, 1977-79, 1988-1990, 2000-2002 and 2012-2014 (Abe et al., 2016, Kochtitzky et al., 2019). Each of these surge events caused the terminus to advance far enough into the valley to fully or partially dam the Dań Zhùr Chù', resulting in the formation of a proglacial lake, generally followed by an outburst flood (Kochtitzky et al., 2020). Since the Little Ice Age maximum extent, Dań Zhùr Glacier has retreated by about 2.5 km (Kochtitzky et al., 2019). This retreat is illustrated in Figure 1.2, which shows that each surge has typically reached a lesser extent than the one before it due to recent retreat caused by a warming climate (Kochtitzky et al., 2019).

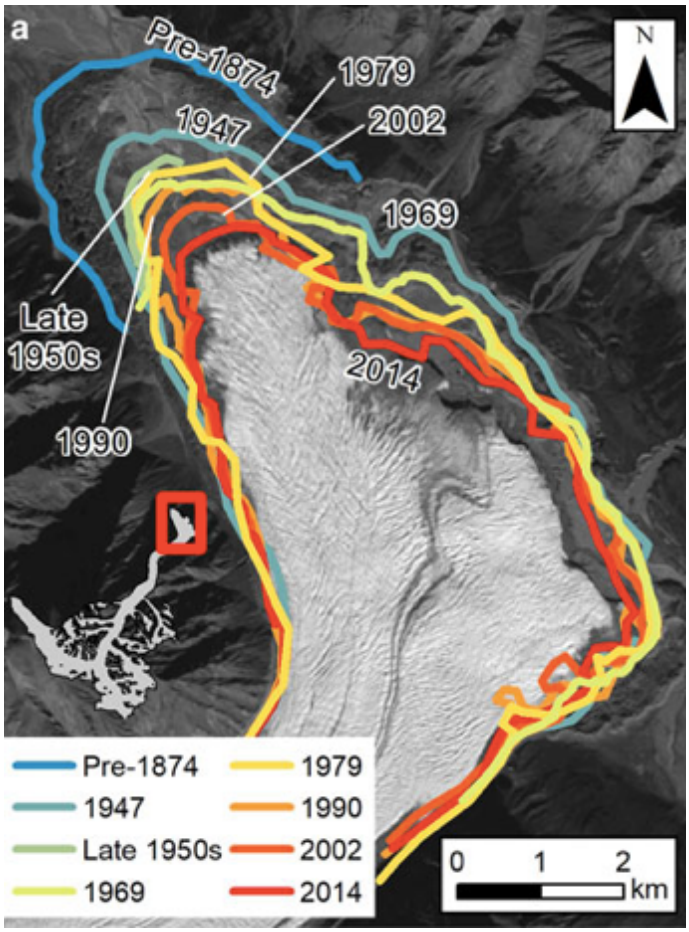

Figure 1.2. Dań Zhùr Glacier terminus position after each surge event, between 1947 and 2014. From Kochtitzky et al., 2019.

To assess historical drainage events, Perchanok (1980) investigated four separate ponding phases of Dań Zhùr Lake by interpreting landforms, vegetation and observed glacial fluctuations. The ponding phases were caused by advance of Dań Zhùr Glacier during the Little Ice Age, with the first episode estimated to have ended between 1470 and 1630 (Perchanok, 1980). The middle two episodes are thought to have been shorter, with a possible duration of about 200 years, but the dates could not be determined. The most recent historical drainage occurred between 1810 and 1840 (Perchanok, 1980). The lakes described by Perchanok (1980) are referred to by Kochtitzky et al. (2020) as Neoglacial Lake Dań Zhùr and are thought to have been much larger than those that have formed more recently, with an area of up to 12.3 km^2.

More recently, work has been undertaken on the surges and lake formation since Neoglacial Lake Dań Zhùr (Abe et al., 2016; Kochtitzky et al., 2019; Kochtitzky et al., 2020). These studies highlight the relatively short surge cycle of Dań Zhùr Glacier of about 12 years

from the beginning of one surge to the beginning of another. Surge type glaciers that experience longer quiescent phases might only surge every 50 to 500 years, which is more common of colder glaciers in areas such as Svalbard (Sevestre & Benn, 2015). Kochtitzky et al. (2020) looked in detail at lake formation during surges of Dań Zhùr since the 1930s and found that the lakes caused by recent surges are larger and drain more rapidly than those prior to the 2000-2002 surge event. This occurs as the retreating glacier leaves behind basins of increasing size between the terminus and the terminal moraine (Kochtitzky, 2020). During a surge event, velocities in the lower 10 km of the glacier have increased by up to two orders of magnitude compared to velocities in the quiescent phase (Kochtitzky et al., 2019). The 2000-2002 velocities were on average higher than the 2012-2014 velocities, with a maximum of 1700 m a^{-1} in 2001 in the lower 3 km of the terminus (Kochtitzky et al., 2019). The average quiescent velocity at Dań Zhùr Glacier is ~130 m a^{-1} (~0.36 m day^{-1}), while the most recent surge event between 2012 and 2014 saw movement of about 3 m day^{-1} over the lower 5 km of the glacier (Kochtitzky et al., 2019).

Julie Cruikshank's book *Do Glaciers Listen: Local Knowledge, Colonial Encounters & Social Imagination*, refers to the surging of Dań Zhùr Glacier and an outburst flood (Cruikshank, 2005). The book describes an account by Chief Albert Isaac in the 1960s, who talks about an incident downstream of Dań Zhùr Glacier that occurred during his lifetime. Two men, out hunting, were crossing the Dań Zhùr Chù' at the end of the day and one was killed by an explosion of ice from an outburst flood upstream (Cruikshank, 2005). These accounts by members of First Nation communities provide important historical context, as they indicate that outburst floods occurred prior to the recent scientific record.

This thesis describes the patterns and mechanisms of the drainages of Dań Zhùr Lake. This expands on the study of Kochtitzky et al. (2020), who primarily looked at the timing of drainage events from Dań Zhùr Lake since the 1930s. Here, the focus is on the mechanism of lake drainage events during the last three surge phases (1988-1990, 2000-2002 and 2012-2014), and their following quiescent periods, as these are the best documented. Before this, some background information is provided about glacial lake outburst floods (GLOFs), as well as the formation and trigger mechanisms of both glacier dammed and moraine dammed lakes.

2.0 Background

2.1 Glacial Lake Outburst Floods (GLOFs)

GLOFs can be particularly catastrophic for downstream populated areas (Hock et al., 2019). Glacier dammed lakes are created when the glacier itself blocks the flow of water, while moraine dammed lakes are caused by the debris left behind as the glacier recedes. A GLOF can occur when the moraine or glacier dam fails, leading to the sudden release of water (Clague & O'Connor, 2015). Glaciers often respond to a warming climate by thinning and receding, which contributes to proglacial lakes by opening more space between the terminus of the glacier and the terminal moraines, consequently allowing increased volumes of meltwater to pool in these areas (Harrison et al., 2018). Globally, the total number of glacial lakes increased by 53% between 1990 and 2018, and the area of these lakes increased by 51% over the same time period (Shugar et al., 2020). The number and area of glacier lakes is expected to increase as glaciers continue to recede in a warming climate, increasing the potential risks of GLOF events (Hock et al., 2019; Shugar et al., 2020).

Glacial lakes can occur at all latitudes and elevations where glaciers are present, which are generally high latitude and/or high-altitude areas. At high altitudes, recent outburst floods have occurred in places such as the Peruvian Andes and the Karakoram (Dussaillant et al., 2009, Chen et al., 2010; Mergili et al., 2020), while in higher latitudes there are many glacier dammed lakes in Alaska/Yukon, Greenland and some in Norway (Russell et al., 2011; Wolfe et al., 2014). Depending on the size of the lake, outburst floods can cause major damage to infrastructure and landscapes at a significant distance downstream (Harrison et al., 2018), and GLOFs are one of the biggest natural hazards in some countries such as Nepal, where many small villages are located at the base of large mountain ranges, where flood waters would track (Yamada & Sharma, 1993). The Intergovernmental Panel on Climate Change states that glacier-related floods have been documented for almost all high mountain areas and are one of the "most far-reaching glacier hazards" (Hock et al., 2019).

2.2 Formation

Water drainage can be hindered in many different areas on and around a glacier (Figure 2.1; Clague & O'Connor, 2015). Meltwater can pool on top or under the glacier, forming

supraglacial and subglacial lakes. Similarly, meltwater can also gather at the terminus (proglacial lakes), glacier margin, or the boundary between two glaciers. Tributary valleys that once were, or still are glaciated, can be an optimal area for water to accumulate, leading to a lake dammed between the tributary and the main valley glacier. The last type of glacier dammed lake is in the main valley when a tributary glacier is advanced far enough to block the drainage of water down the valley; this appears to be the main way in which recent dams have been formed by Dań Zhùr Glacier (type H in Figure 2.1), as the glacier has dammed water in the main valley coming from Kluane Glacier and other ice masses upstream.

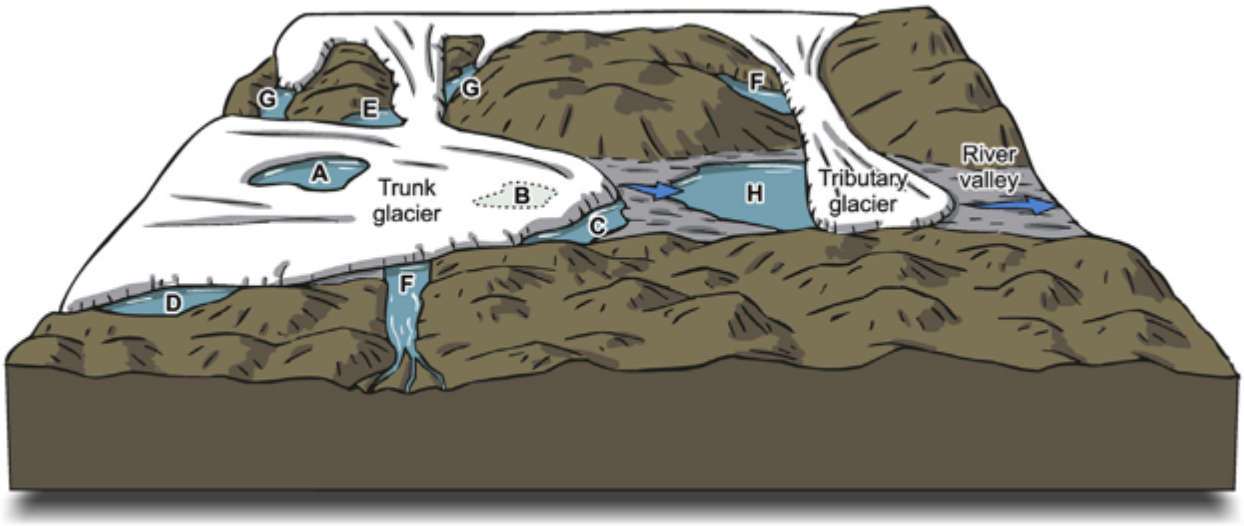

Figure 2.1. Locations where water can be dammed by a glacier: A) supraglacial, B) subglacial, C) proglacial, D) embayment in slope at glacier margin, E) at coalescence of two glaciers, F) tributary valley adjacent to a trunk or tributary glacier, G) tributary valley dammed on both sides of the lake, and H) main valley adjacent to a tributary valley. From Clague & O'Connor, 2015.

Moraine deposits consist of loose, unsorted sediment transported within, at the base, or on top of a glacier. These deposits can accumulate at the terminus of the glacier and are left behind as mounds when the glacier recedes. Some moraines are ice-cored and consist of only a small layer of sediment, while others contain only minimal pore ice, or no ice at all (Clague & Evans, 2000). A moraine-dammed lake is caused by an end-moraine acting as a barrier to glacier meltwater, with the end moraines of many present-day glaciers being formed during the Little Ice Age, which peaked in ~1874 at Dań Zhùr Glacier (Denton & Stuiver, 1966).

2.3 Trigger mechanisms: glacier-dammed lakes

There are many different trigger mechanisms that can cause a glacier dam to fail. Over spilling occurs when the water in the lake gets high enough to spill over the glacier dam. This is more common in cold-based glaciers that are frozen to the bed and resistant to water passing between the ice and the underlying rock or sediment (Maag & Müller, 1972). Over spilling may also occur when a large volume of ice or debris falls into the lake, creating a wave that can overtop the dam (Iturrizaga, 2011).

Flotation of the dam is another mechanism of drainage. Depending on the density of the ice (which can be altered by debris content) the glacier dam can begin to float when the water column reaches a height of about 90% of the ice thickness (Björnsson, 2009; Knight & Russel, 1993). This can be a cyclic event - water drains during flotation and once the lake reaches a lower level the glacier dam sinks to block the water flow once again. The lake then begins to refill until the water reaches an adequate height to create the buoying effect, and the cycle begins again (Iturrizaga, 2011). This mechanism has been observed at an ice-marginal lake in the ablation zone of Kaskawulsh Glacier in the Yukon (Bigelow et al., 2020). When the lake drained, the glacier re-grounded, allowing the lake to refill and commence the process again (Bigelow et al., 2020).

Another explanation for drainage from some ice-dammed lakes has been termed the Glen mechanism (Glen, 1954). When the water pressure of a lake exceeds that of adjacent ice (similar to the flotation mechanism above), the outflow carves out a subglacial channel, causing drainage of the lake (Glen, 1954; Higgins, 1970). Once the subglacial channels are opened, additional frictional melting occurs, enlarging the channels and allowing faster drainage (Iturrizaga, 2011).

A different mechanism of drainage caused by deformation to the ice dam itself is subaerial breach-widening. This refers to a sudden rupture or detachment of the glacier dam, which generally leads to very rapid drainage of the lake (Walder & Costa, 1996). The breach widening is assumed to be controlled by melting and can occur following the collapse of a tunnel roof (Walder & Costa, 1996)

Two of the less common trigger mechanisms are volcanic and seismic activity. Subglacial volcanic activity creates geothermal heat, which can thin an ice dam and accelerate drainage, or can breach the dam altogether (Björnsson, 1992). Iceland is one of the most common areas for jökulhlaups, which is the Icelandic term for GLOFs caused by volcanic

activity, as ~60% of the glaciers in the country occur in an active volcanic zone (Björnsson, 1992). A very well studied case of jökulhlaups is that of the subglacial lake Grimsvötn, located under Vatnajökull in southern Iceland (Jóhannesson, 2002). The main cause of these events is due to melting of ice underneath the glacier as a result of geothermal heat, causing water to settle into a depression, accumulating until it reaches a critical level, and an outburst flood occurs (Björnsson, 1974, 1992). A significant outburst event from the southern margins of Vatnajökull in 1996 was caused by a subglacial volcanic eruption from Grimsvötn, leading to an abrupt jökulhlaup with discharge rates reaching about 40 x 10^3 m^3 s^{-1} (Jóhannesson, 2002).

Seismic activity is not a common cause of GLOFs, but similarly to subaerial breach-widening, it can result in a large scale, rapid drainage (Iturrizaga, 2011). In 1918 a very large jökulhlaup occurred when the Icelandic subglacial volcano Katla erupted (Tómasson, 1996). The eruption was strong enough to cause an earthquake and was followed by breaching of the glacier dam and draining of the lake. Several cubic kilometers of water flowed from the glacier into the sea, transporting volcanic material, and icebergs from the dam (Tómasson, 1996).

2.4 Trigger mechanisms: moraine-dammed lakes

As with glacier-dammed lakes, there are several trigger mechanisms for moraine-dammed lakes, many of which are illustrated in Figure 2.2. Ice, snow or rock debris can cause a large displacement wave to overflow or carve out a section of the moraine, leading to rapid drainage (Figure 2.2 E; Iturrizaga, 2011). This can be common as processes such as calving, ice falls and avalanches occur from nearby hanging glaciers, and is thought to be the cause of many GLOFs in the Andes and Karakoram mountains (Somos-Valenzuela et al., 2016).

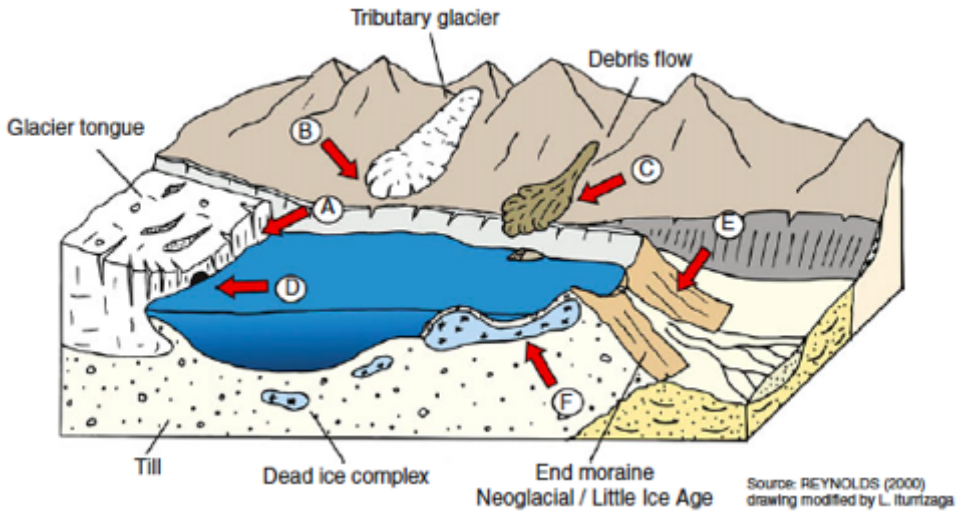

Figure 2.2. Moraine dammed lake and potential triggers for release. A) calving, B) avalanches, C) debris flow, D) sudden meltwater drainage, E) dam failure, and F) ice-cored moraine melt. From Iturrizaga, 2011.

There have been catastrophic GLOFs in the past, more so in low to mid-latitude mountain areas where populations and infrastructure are more established. An extreme example is the rupture of Palcacocha Lake in the Cordillera Blanca mountains of Peru. On December 13th, 1941, the dam breached, resulting in a debris slide that killed thousands of people in the city of Huaraz (Klimeš et al., 2016). Although the exact cause of the breach is not known, it is thought to have been an ice fall from a surrounding mountain or weakening of the moraine through erosion (Klimeš et al., 2016). This tragic event sparked an effort for glacier dam reinforcement in the Cordillera Blanca and increased monitoring of glacier and moraine dammed lakes in the region.

Ice-cored moraines are a significant concern in the currently warming climate (Clague & Evans, 2000), as melt or thaw can destabilize the moraine, and if the ice core is large, the meltwater can even contribute to the volume of the lake (Figure 2.2 F; Iturrizaga, 2011). Similar to glacier-dams, volcanic eruptions and large earthquakes can displace moraine material and weaken the dam, allowing water to break through and subsequently drain (Iturrizaga, 2011). Changes in the drainage of a glacier or associated moraine can also cause outburst floods. For example, sudden large-scale drainage from within or under the glacier can supply large volumes of water to a lake, causing an overflow or destabilization of the dam (Iturrizaga, 2011). If the moraine contains its own drainage system, these channels or seeps can be enlarged, causing water to drain more rapidly, or break through the moraine entirely (Iturrizaga, 2011). Another

factor that can contribute to an increase in lake level is heavy rainfall events or large/rapid snowmelt throughout the melt season (Iturrizaga, 2011).

In Canada, moraine-dammed lakes are not as well understood as those in the Alps or Andes, as the remote locations and lack of population in Canadian mountain regions mean that these events tend to go unnoticed (Clague & Evans, 2000). However, as development and mining increase in the Canadian mountains, more information is needed on moraine-dammed lake processes to understand any potential hazards. Clague and Evans (2000) conducted a review of various moraine dam failures in western Canada. In this area, glaciers began retreating from their Little Ice Age extent at the end of the 19th century, and many lakes formed between the retreating glacier and their end moraine. Two of the moraine dam failures in British Columbia studied by Clague and Evans (2000) were attributed to overtopping caused by ice avalanches. As previously mentioned, this is thought to be one of the most common failure mechanisms in mountainous environments, as many glaciers have retreated up steep slopes and are prone to crevassing and failure.

Another recent example of a moraine dammed lake drainage was at the terminus of Kaskawulsh Glacier, ~65 km south of Dań Zhùr Glacier (Shugar et al., 2017). The lake, named Slims Lake, formed and grew as the glacier retreated, and between 2000 and 2015 the lake increased in size by more than three times (Shugar et al., 2017). In the summer of 2016, a channel was established through dead ice at the terminus of the glacier and was enlarged by meltwater and localized collapse of the channel walls, resulting in a rapid drop in lake level by 17 m (Shugar et al., 2017). This significant lowering of Slims Lake caused the drainage to re-route from its previous northward direction into Łù'àn Män (Kluane Lake), to southward into the Kaskawulsh River and then Alsek River (Shugar et al., 2017). The discharge from Slims Lake was previously the main input to Łù'àn Män, meaning that the Yukon's largest lake lost its primary supply of water. The annual water level variations of the Łù'àn Män have decreased from 2 m to 0.5 m, and the minimum winter levels are now about 0.25 m lower than prior to the river re-routing (McKnight et al., 2021). This has influenced sediment load, nutrient flux, fish populations and lake drainage (Shugar et al., 2017).

2.5 Historical Dań Zhùr Lakes

A study was undertaken on the historical draining and filling of Dań Zhùr Lakes by Kochtitzky et al. (2020). Their paper provides the details of lake formation, as well as the timing of lake filling and draining, since the 1930s, by using historical air photos and more recent satellite imagery. The formation of these lakes is driven by glacier surges, which occur approximately every 12 years at Dań Zhùr Glacier (Kochtitzky et al., 2020). A surge-type glacier is characterized by cyclical variations between long periods of slow flow during the quiescent phase, followed by short periods of much faster flow during the active phase. Although the duration of the active and quiescent phases varies widely, they appear to be relatively consistent for each individual glacier (Meier & Post, 1969). The surge cycle of warm-based glaciers commonly lasts for 2-3 years, while the quiescent phase generally ranges between 20-30 years (Meier & Post, 1969). At Dań Zhùr Glacier the surge cycle is generally about 2 years and the quiescent cycle about 10 years. Alaska and Western Canada contain one of the highest concentrations of surge-type glaciers in the world, with 113 confirmed (Sevestre & Benn, 2015). On the Canadian side of the St. Elias Mountains, Clarke et al. (1986) estimated that ~6.4% of the glaciers are surge-type, but more surge-type glaciers have been identified in this region since their study.

Historical air photos provide some insights into surge events and lake formation prior to the 1977-1980 surge event. During this time, Dań Zhùr Glacier was larger in size and therefore surge events advanced further into the valley. The greater extent of the ice in the valley made it difficult for large lakes to form. A historical air photo from 1947 shows the Dań Zhùr Glacier at its most advanced position on record and indicates that Dań Zhùr Chù was relocated to the North side of the valley as the glacier advanced, and therefore avoided being dammed by the ice (Kochtitzky et al., 2020).

Small proglacial lakes were displaced by the onset of the 1950s, ~1969, 1977-1980 and 1988-1990 surge events (Kochtitzky et al., 2020). Following the 1988-1990 surge, a lake was not observed to form at the terminus until 1993, when a small lake formed in a basin exposed by the retreat of Dań Zhùr Glacier. This lake increased in size, and other small lakes formed in other areas of the terminus, until fall 1997, when part of the largest lake drained, leaving it with an area of 0.32 km^2, about a third of its original size (Kochtitzky et al., 2020). In the spring of 1998, the rest of the lakes drained and no lakes formed until the next surge event. The presence of this

canyon did not allow any lakes to form until the next surge event, which began in 2000 (Kochtitzky et al., 2020).

In summary, glacier and moraine dammed lakes occur all over the world, particularly in high altitude and high latitude regions, and GLOF events from these lakes are expected to be an increasing phenomenon as continued climate warming leads to increased meltwater from these glaciers (Hock et al., 2019; Shugar et al., 2020). Once a glacial lake has formed, GLOFs can occur through many different trigger mechanisms, such as overspilling or flotation, among others. In Western Canada many of these outburst events occur in remote mountainous areas, but as development continues to increase, these events could lead to dangerous and damaging flooding events (Geertsema & Clague, 2005). In the following chapter the methods are discussed that were used to understand past GLOFs at Dań Zhùr Glacier since 1988, with the findings used in later chapters to provide insight into what might occur there in the future.

3.0 Methods

This chapter describes the data and methods used to determine the causes, patterns, and mechanisms of the drainage of Dań Zhùr Lake, over the last three surge cycles since 1988, building on Kochtitzky et al. (2020) which provided information on the timing of historical drainage events. The data presented in this chapter include information from aerial photos, satellite images, digital elevation models, and field observations. These data are used to examine temporal changes in glacier and lake extent and volume, and their connection to glacier surging, along with the causes and routing of past lake drainage events, and how these are changing under a warming climate. In later chapters this information is used to provide a better understanding of the mechanics of GLOF drainage events, potential hazards posed by these events in the SW Yukon, and future implications for their occurrence.

3.1 Datasets

3.1.1 Historical aerial photography

Aerial photographs (Table 3.1 and Figure 3.1) are used to provide historical context for the recent changes at the terminus of Dań Zhùr Glacier and Dań Zhùr Lake. The earliest aerial photo, from 1937, was taken by Bradford Washburn and was acquired from the Alaska and Polar Regions Collections and Archives at the Elmer E. Rasmuson Library at the University of Alaska Fairbanks (UAF). Because these photos were oblique, they were not georectified. Another set of photos from 1961 to 1969 by Austin Post were obtained from the University of Washington (UW) Special Collections, and finally photos taken by the Royal Canadian Air Force (RCAF) in 1947, 1956, 1977 and 1978 were acquired from the Yukon Energy, Mines, and Resources Library in Whitehorse, Yukon. These photos were nadir, and georectified in ArcGIS using tie-points and a high-resolution Worldview-2 image from September 2, 2012.

Table 3.1. Description of historical aerial photographs used in this study.

Photo ID	Date Acquired	Taken By	Source
wb0516	14 August 1937	Bradford Washburn	University of Alaska Fairbanks
PHColl734, YD24	1961	Austin Post	University of Washington
PHColl734, YD32	25 August 1968	Austin Post	University of Washington
PHColl734, YD37	27 August 1969	Austin Post	University of Washington
A11002-274	24 July 1947	RCAF	Yukon Government
A15434-179	10 August 1956	RCAF	Yukon Government
A24758-088	27 July 1977	RCAF	Yukon Government
A24952-022 to 25	3 July 1978	RCAF	Yukon Government

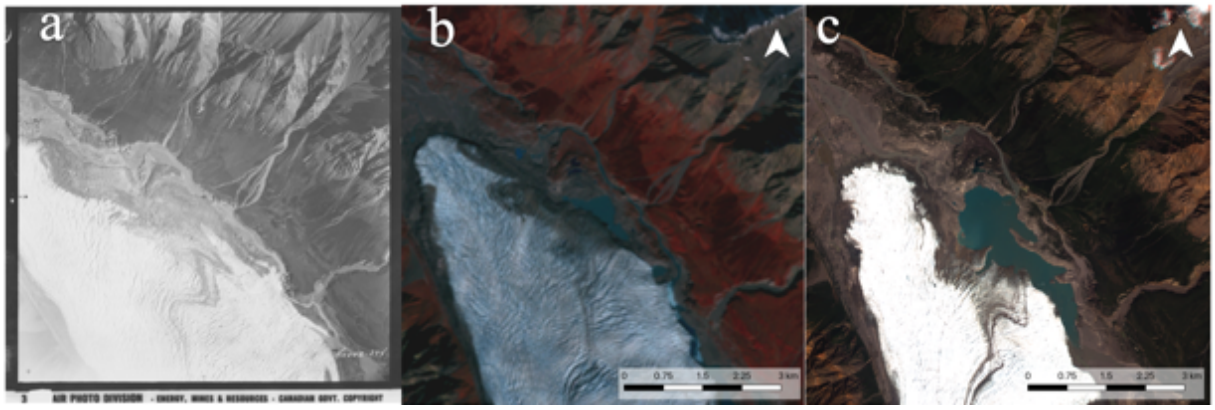

Figure 3.1. Example of historical aerial photo and satellite images of the terminus of Dań Zhùr Glacier: a) 24/07/1947 RCAF (A11002-274); b) 15/09/2002 Landsat 7; c) 06/07/2019 Planet.

3.1.2 Satellite imagery

For the period ranging between the 1970s and 2020, satellite scenes were acquired from Landsat-5, 7 and 8 (15-30 m resolution), ASTER (15 m), Sentinel-2A (10 m) and Planet (3-5 m) sensors. The imagery was preferentially acquired during snow-free months (May-September), and during periods of lake formation and drainage. The Planet satellite images were sourced from the Planet Labs website (https://www.planet.com/) under their Education and Research Program, while all others were sourced from the United States Geological Survey (USGS) Earth Explorer database (https://earthexplorer.usgs.gov/). Planet was the main source used for imagery

since the 2014 surge due to its high resolution and high temporal repeat daily coverage, while imagery prior to that was sourced primarily from Landsat. The Landsat imagery is the oldest, dating back to 1973, and therefore covers the last three surge events.

3.1.3 Field measurements

For the most recent drainage event of Dań Zhùr Lake in summer 2019, aerial photo surveys were undertaken across the glacier, lakebed and downstream areas on June 30th and September 6th, 2019 (Figure 3.2). These surveys used a Nikon D850 45-megapixel camera with a 24 mm lens, which captured nadir photos every 3 seconds (Figure 3.3). The unit was mounted in a Helio Courier aircraft operated from Silver City Airfield, approximately 20-minute flight time from Dań Zhùr Glacier. The GPS positions of the photos were recorded with a Trimble R7 differential global positioning system (dGPS) system by using an electrical impulse triggered by the camera flash mount (hot shoe) to place a marker in the dGPS record.

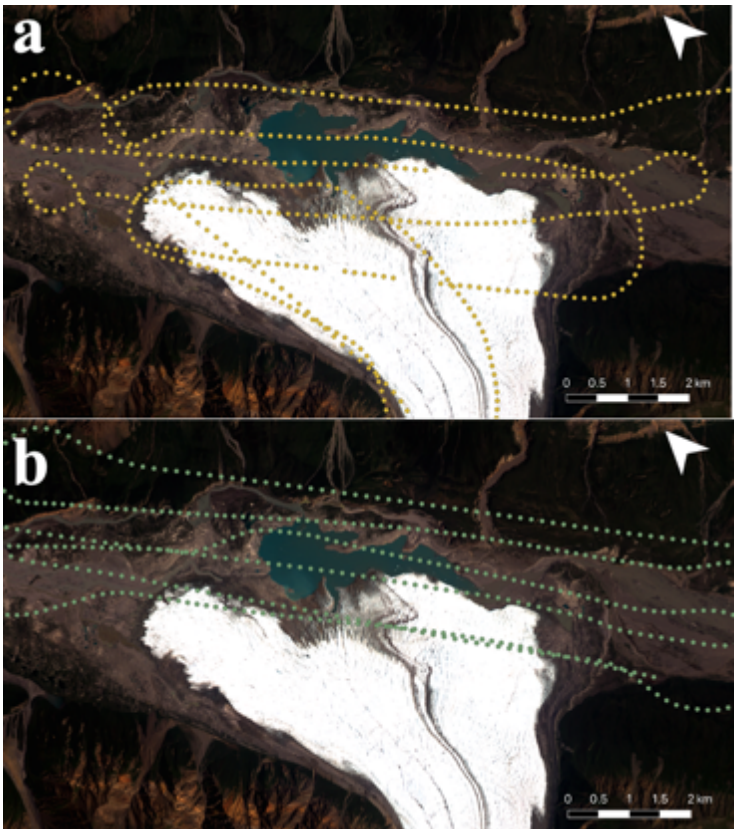

Figure 3.2. 2019 aerial photo flight track across the terminus of Dań Zhùr Glacier; a) June 30, 2019, and b) September 6, 2019; (Base satellite image: Planet, 2019-07-06).

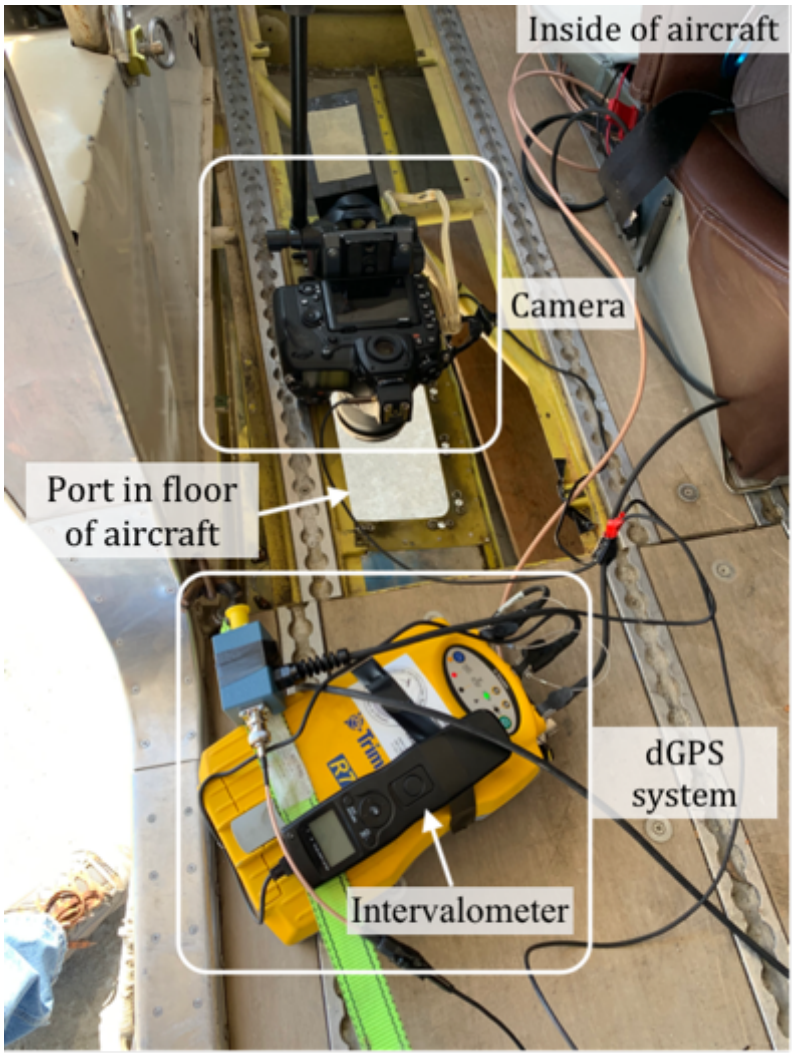

Figure 3.3. Set up of camera equipment inside Helio Courier aircraft for air photo surveys in 2019.

An Onset HOBO U20-001-01 Water Level logger (https://www.onsetcomp.com/products/data-loggers/u20-001-01/) was lowered into the edge of Dań Zhùr Lake on July 12th, 2019, which captured the drainage event that summer (Figure 3.4a). The logger settled on a small hill in the lake and therefore did not reach the bottom of the lake. For this reason, the full drainage was not recorded, but the existing pressure sensor data were used to confirm the timing and duration of the 2019 lake drainage for the time that it was submerged, as well as the change in water depth, and therefore drainage rate, of the lake. Absolute pressure measurements were taken every 30 minutes, with an accuracy of 0.62 kPa. The sensor was retrieved on September 5, 2019.

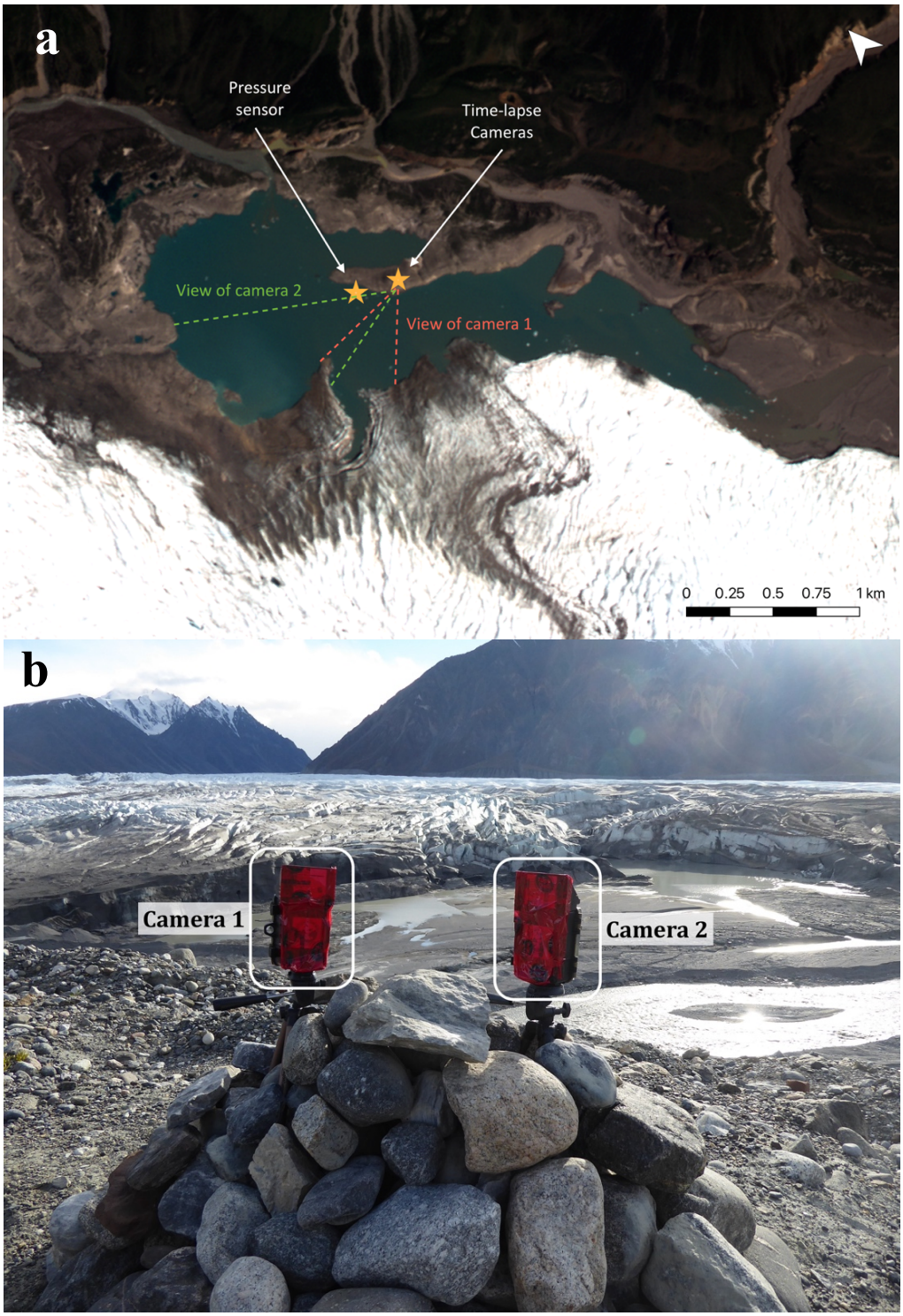

Figure 3.4. a) Location of pressure sensor and time-lapse cameras at the terminus of Dań Zhùr Glacier (Base satellite image Planet 2019-07-06); b) View of time-lapse cameras overlooking the terminus of Dań Zhùr Glacier on August 31, 2020.

The 2019 drainage event was also captured by two SpyPoint Solar Trail cameras (https://www.spypoint.com/en/support/solar-trail-camera/product-solar.html). These cameras were installed on small tripods on bedrock in front of the terminus of Dań Zhùr Glacier on July 12, 2019, capturing the subsequent lake drainage, and photos were retrieved on September 5, 2019. The cameras recorded images hourly, facing in two different directions towards the terminus of the glacier. The east facing camera 1 pointed directly at the front of the glacier, while the west facing camera 2 was angled towards the area where an ice canyon formed shortly after the 2019 lake drainage event (Figure 3.4).

An ablation pole was drilled into the ice near the terminus of Dań Zhùr Glacier on July 12th, 2019, along with a time-lapse camera, to determine glacier melt. Stripes were marked on the pole with the use of 5 cm wide coloured tape, which enabled the determination of accumulation and ablation rates from hourly pictures (Figure 3.5). These images were used to get an estimated daily melt rate at the glacier terminus in the summer of 2019.

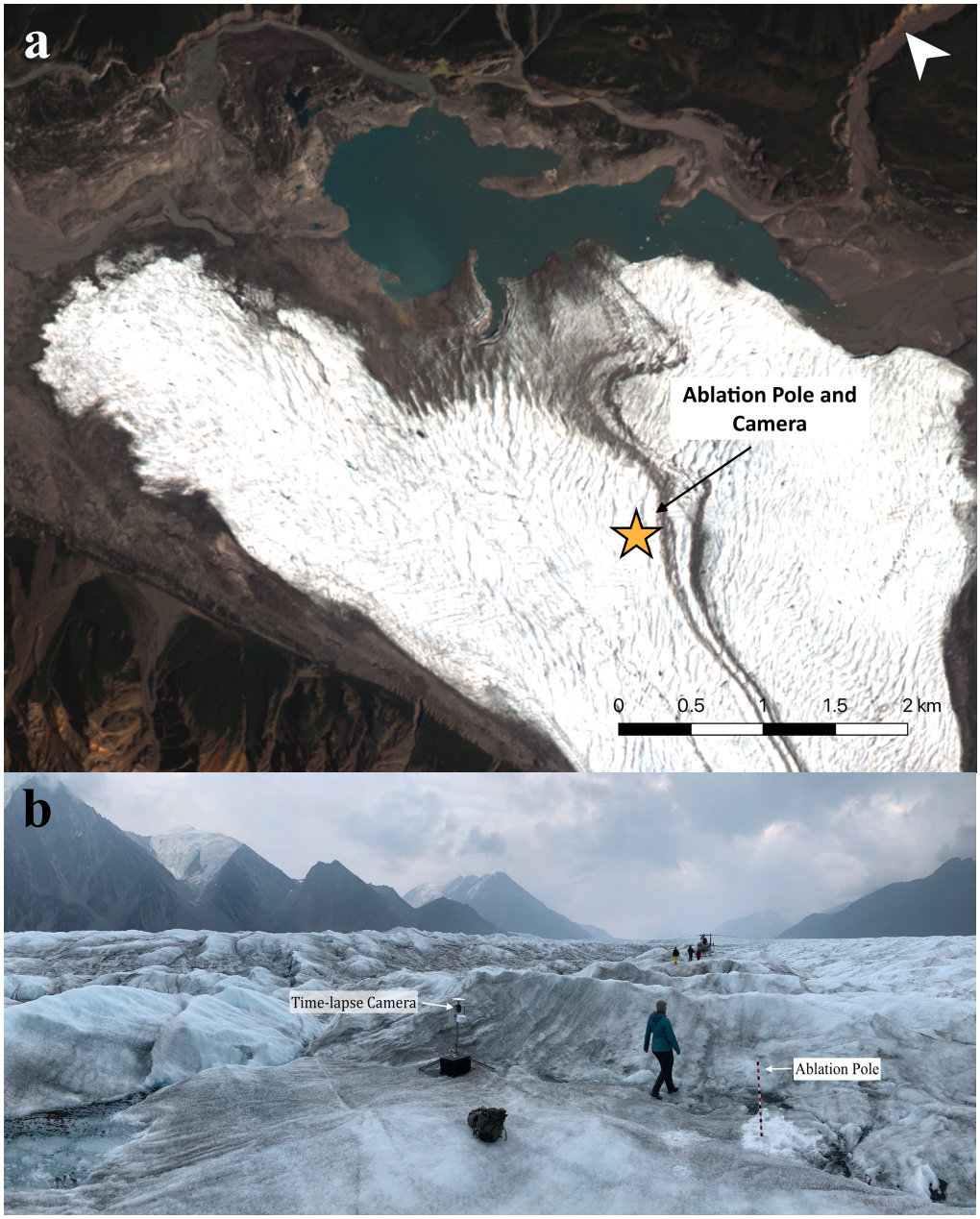

Figure 3.5. a) Location of the ablation pole and time-lapse camera on the terminus of Dań Zhùr Glacier (Base satellite image: Planet, 2019-07-06); b) Ablation pole and GPS near the terminus of Dań Zhùr Glacier on July 12, 2019.

3.2 Analysis of Datasets

3.2.1 DEMs

The photos acquired from the two aerial photo surveys were used to construct high-resolution digital elevation models (DEMs) and orthomosaics using Structure from Motion (SfM) techniques (Figure 3.6) with the software Agisoft Metashape Professional. The dGPS data

collected with the Trimble R7 during each survey were processed using the Precise Point Positioning (PPP) service of Natural Resources Canada (https://webapp.geod.nrcan.gc.ca/geod/tools-outils/ppp.php), which enables reconstruction of the accurate position of the dGPS receiver from precise orbital information that is released approximately 12 days after data acquisition. This allows for positioning of the GPS receiver to an accuracy of a few cm or less, without the need for a ground station. A custom Python script, written by Will Kochtitzky, University of Ottawa, calculated a linear interpolation between known dGPS points to find the position of the photograph relative to a given event marker in the dGPS record.

The raw photos captured during the aerial photo surveys were loaded into the Agisoft software, together with their location determined from the dGPS data. After inspection, any unnecessary images were deleted, such as edge photos where the plane was turning and photos from up-glacier locations that were outside the area of interest. The remaining photos and their positions were then processed to produce a sparse point cloud, which is a 3D representation of the tie-point data, involving feature point detection and matching procedures (Agisoft, L.L.C, 2020). After producing the sparse point cloud, the next step generated depth information for each photo using the photo positions and displayed it in a single dense point cloud. From this dense point cloud data, Agisoft Metashape was used to produce a DEM, which represents a surface model as a regular grid of height values (Agisoft, L.L.C, 2020). An orthomosaic was also produced in Agisoft Metashape, which consists of a seamless high-resolution image of the area of interest obtained by orthorectifying and stitching together the original images.

Because the DEMs were produced at different resolutions (Table 3.2), they were resampled to a standard resolution of 2 m to allow for consistency during the co-registration process. The DEMs were co-registered to minimize vertical displacement over stable ground. This was achieved using a Python script from Shean et al. (2016) to enable horizontal and vertical alignment of DEMs. The September 2019 DEM was co-registered to the June 2019 DEM to enable calculation of differences over the lake and glacier areas caused by the lake drainage event (Figure 3.7).

Table 3.2. Details of DEMs constructed from 2019 air photo flights over Dań Zhùr Glacier terminus.

	June 30, 2019	**September 6, 2019**
# of photos (terminus)	437	533
DEM resolution (cm)	44.3	24
Total estimated error (cm)	500.2	500.4

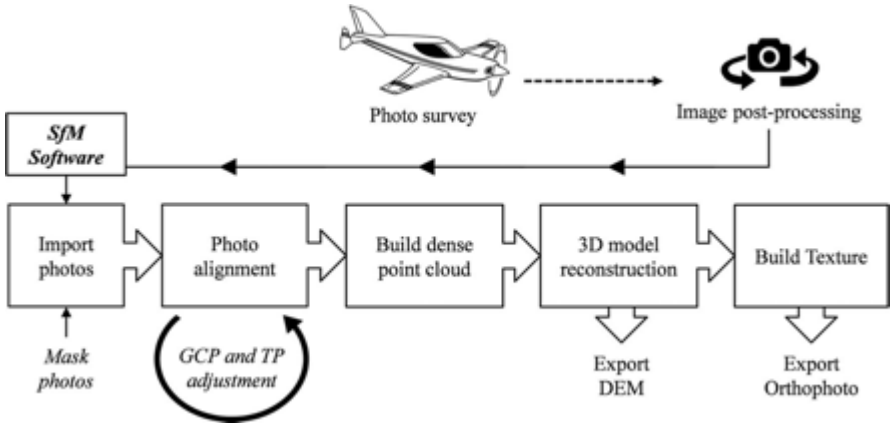

Figure 3.6. Workflow for creating a DEM using the photogrammetry software Agisoft Metashape Professional. From Thomson & Copland (2016).

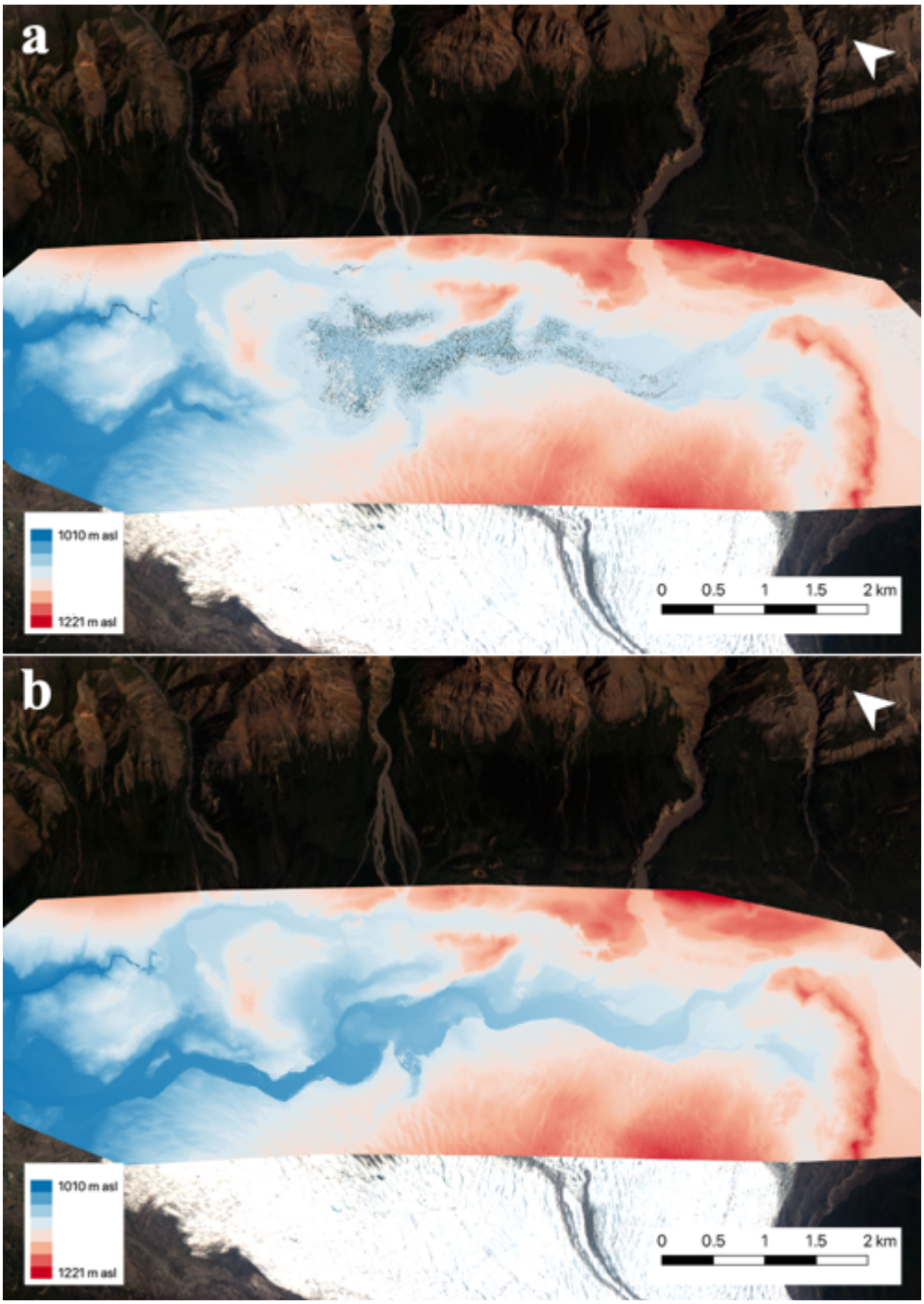

Figure 3.7. DEMs of the terminus of Dań Zhùr Glacier and Dań Zhùr Lake from June 30th, 2019 (a) and September 6th, 2019 (b), after co-registration.

3.2.2 Lake area and volume

The co-registered DEMs were used alongside satellite imagery to determine lake area and volume. Satellite images of Dań Zhùr Lake from shortly before its drainage in 2017, 2018 and 2019 were manually outlined, using QGIS3.4, to create a shapefile of each lake. These satellite images were sourced from Planet and were from July 7th, 2017, August 18th, 2018, and July 6th, 2019. The assumption was made that the lakebed remained stable over this three-year period due to limited time for erosional processes.

Lake area was calculated in QGIS, using the "Zonal Statistics" tool, under "Raster Analysis." This tool provides various statistics values for a raster layer within the zone of a vector layer. In this case, the raster layer was the September 2019 DEM, and the vector layer was either the 2017, 2018 or 2019 lake outline shapefile. The statistical value used to calculate lake area was the pixel cell count, which was the number of pixels within the lake outline. This number was multiplied by 4 m^2, which was the size of each pixel, in order to determine the entire area of the lake in m^2.

The lake volume was calculated in ArcMap 10.6.1 using the same lake outlines and DEMs as were used in the area calculation. Using the lake outline of the year in question, the tool "Points along geometry" was used to create a new shapefile with points spaced every 5 m along the lake outline. This was applied in order to obtain a representation of lake elevation values along the shoreline. The "Sample raster values" tool was then used to extract the elevation values for each point, and these were averaged to get an average lake elevation height. This assumes that the lake surface is flat across the region of interest. The next step in the lake volume process was to use the "Extract by mask" tool to clip the September DEM of the lakebed to the extent of the lake before it drained in that year. Once these steps were complete, the resulting datasets included both a lake elevation value, as well as a lakebed DEM of the respective year. With these values, the lake volume was calculated using the "Surface Volume" tool. This tool allows for the calculation of volume of a surface, either above or below a reference plane. In this case, the volume was calculated using the cropped lakebed DEM as the surface, below the reference plane of the average lake elevation.

3.2.3 Drainage timing

The estimated timing of the drainage of lakes that formed over the last three surge cycles was primarily determined using satellite images, although in 2019 we were able to obtain more accurate details using the time-lapse cameras and the pressure logger. The pressure logger data were used to determine a rate of water depth change in m/s. The raw data was recorded in units of kPa, so in order to convert into meters of water head, it was multiplied by 0.101972 (https://www.sensorsone.com/kpa-to-mh2o-conversion-table/). The rate of change of lake level was then determined by subtracting each value from the value recorded ½ hr previously, and then dividing by 1800 to convert from meter per ½ hour to meter per second. There was one outlier, at 4:30 am on July 13th, 2019, that showed the rate of change to significantly slow down by 0.24 m/h when all surrounding data points showed a steady, higher rate of drainage, so it was removed.

3.2.4 Drainage routes

Drainage routes were determined using Planet and Landsat imagery. Images were downloaded and loaded into QGIS for the time before and after each lake drainage for the past three surge cycles (i.e., since 1988) in order to determine at which location the lake drained. The drainage location was determined by examining the "after drainage" image for the route of the river, either through, under or around the terminus of the glacier once the lake was empty. A second indication of drainage location was the gathering of icebergs in one part of the lake prior to drainage, due to water currents drawing icebergs to that spot.

3.2.5 Terminus position

Satellite imagery was used to determine the change in terminus position of Dań Zhùr Glacier throughout different surge events. The terminus position at its maximum surge extent, and minimum quiescent extent, were mapped for last three surge events in 1988-1990, 2000-2002 and 2012-2014. Satellite imagery was sourced from Planet for the years 2012-2019, and the USGS for the years prior to 2012. Landsat 7 imagery was used for the 2002 surge extent and the 1999 quiescent extent, and Landsat 5 imagery was used for the 1990 surge extent. The terminus positions were traced using this satellite imagery in QGIS.

3.2.6 Flotation

In order to determine which areas of the glacier terminus were likely to float at the maximum lake depth in 2019, a calculation was undertaken based on the difference in density between ice (~917 kg/m^3) and water (~1000 kg/m^3) (Shumskiy, 1960).

$$If\ L > 0.917i,\ then\ flotation\ will\ occur$$
$$L = Depth\ of\ Lake$$
$$i = Ice\ thickness$$

This calculation was based on the assumption that if the water column of the lake was more than 91.7% of the ice thickness at the front of the glacier, then flotation of the ice would occur. Some error in this calculation may come from the density of ice, as it was assumed that the ice at the terminus was pure, whereas in reality the density can vary depending on other factors such as temperature and the amount of debris within the ice.

The 2019 DEMs created from the aerial photos were used to extract elevation values for the glacier surface, empty lakebed, and the full lake; ice thickness and water level were then calculated by subtracting the lakebed elevation from the glacier surface elevation or full lake elevation, respectively. The ratio of 91.7% of ice thickness to water level was used to classify the margin of the glacier, so that areas with a value of > 1 were marked as floating, and areas with a value of < 1 were marked as not floating. Finally, these data were imported into QGIS to plot the areas of flotation/no flotation on top of a satellite image for visual comparison.

3.3. Summary

These data and methods were used to determine the causes, patterns, and mechanisms of the drainage of Dań Zhùr Lake over the last three surge cycles since 1990. Datasets including aerial photos, satellite images, and field observations were collected and processed to provide details on terminus and lake elevation and extent, lake drainage paths and timing of these events, and how these are changing over time. The results from these data are outlined in the next chapter and are then used to discuss how this provides a better understanding of the mechanics of GLOF drainage events, potential hazards posed by these events, and future implications for their occurrence.

4.0 Results

This chapter describes the results concerning the causes, patterns, and mechanisms of the drainage of Dań Zhùr Lake over the last three surge cycles since 1988-1990. It starts by presenting two of the historical surges, 1988-1990 and 2000-2002, to outline the terminus changes and lake activity during and after the surge events. Similar information is then presented about the most recent surge event, 2012-2014, and the following quiescent phase. Following this, more detail is provided about the 2017, 2018 and 2019 drainage events, such as the causes of the 2019 drainage event and its connection to flotation of the glacier terminus, and the drainage routes of past events and changes in past terminus position. Based on data availability, the descriptions of earlier events are less detailed than those of more recent events, particularly for 2019 where direct field observations enable a comprehensive account of what occurred.

4.1 Drainage events since 1988-1990 surge

From the onset of the surge in 1988 to the end in 1990, the terminus of Dań Zhùr Glacier advanced by an average of 377 m to cover the basin where lakes had formed during the previous quiescent phase. After this advance, no new lake developed until the summer of 1993, about three years after the start of the quiescent phase. At that time some very small lakes, less than 0.1 km^2 in area, appeared (Figure 4.1), and the following year a lake began to develop in a basin at the southeast side of the terminus, which slowly expanded to reach 0.65 km^2 by 1996 (Kochtitzky et al., 2020). Following this, a new lake formed to the north end of the terminus and then subsequently drained into the lake that was already present, creating an even larger southern lake with an area of ~0.9 km^2 (Figure 4.1). In the fall of 1997, a portion of this lake drained reducing its area to 0.32 km^2 (Kochtitzky et al., 2020). In spring 1998, the remainder of the lake drained through a subglacial channel which eventually collapsed to form an ice canyon through the terminus of the glacier, preventing the lake from forming again until after the next surge event (Kochtitzky et al., 2020). Between 1990 and the end of the quiescent phase in 1999, the glacier retreated by an average of 602 m, and up to a kilometer in some areas, allowing meltwater to form lakes in basins exposed by the retreating terminus.

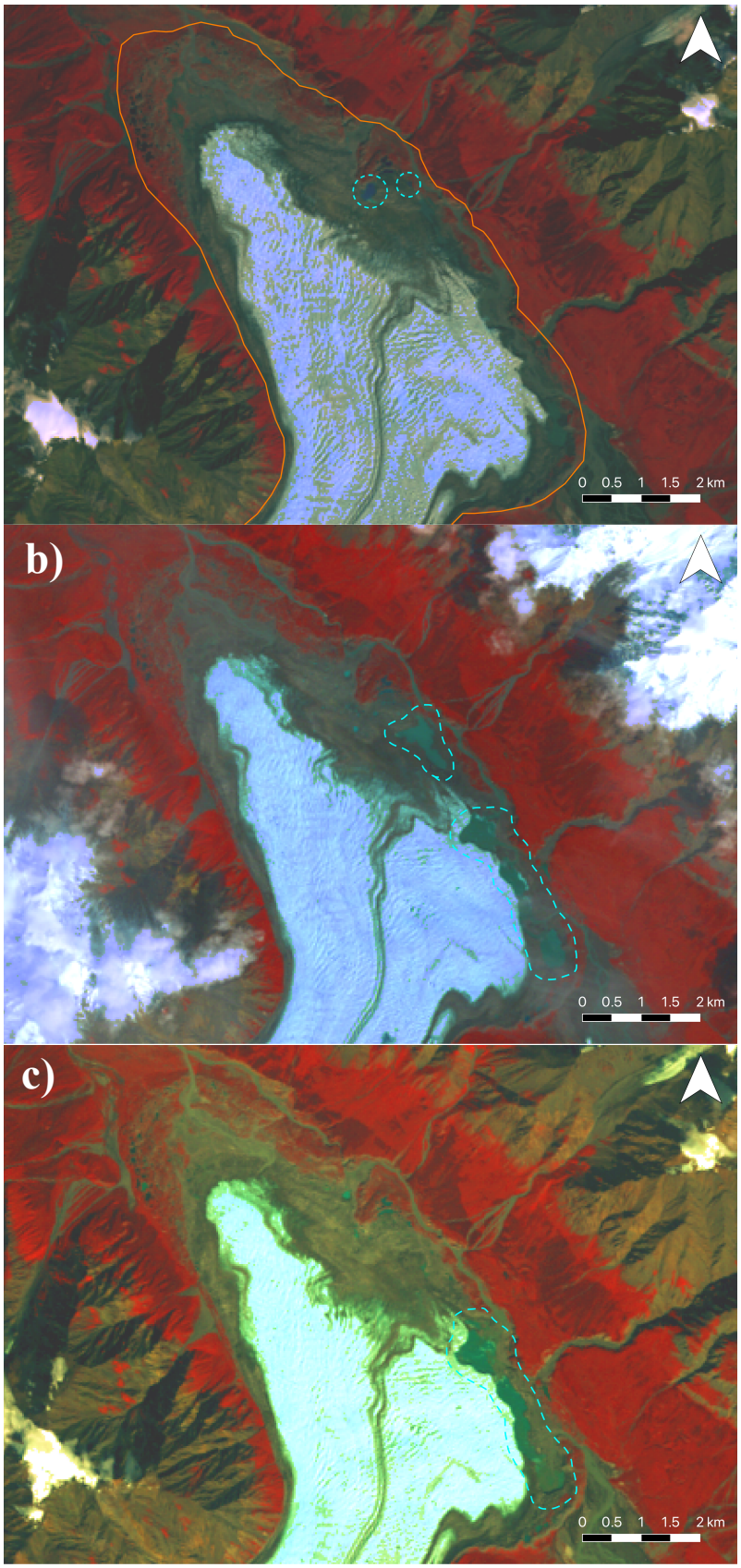

Figure 4.1. Dań Zhùr Lakes on a) 28 July 1993; b) 4 July 1996; and c) 15 August 1997 (Landsat 5). Blue dashed lines represent an area where there is a lake present. Orange line in figure a) is Neoglacial maximum moraine.

4.2 Drainage events since 2000-2002 surge

The next surge event began in the winter of 2000 and lasted until the fall of 2002, during which time the terminus of Dań Zhùr Glacier advanced by an average of 354 m. Between 2000 and 2002, several small lakes appeared at the terminus as the advancing glacier began to block the Dań Zhùr Chù. These lakes drained before the end of the surge event, but by the end of the melt season, in September 2002, another lake had begun to form and grew to an area of 0.68 km^2 (Figure 4.2) (Kochtitzky et al., 2020). The lakes grew to reach about 1.17 km^2 in the summer of 2003, and then persisted through 2004 and 2005, with some small fluctuations in size. By the 23rd of June 2006, there was a northern lake and a southern lake that together totalled 1.12 km^2 in area, but by the end of the month, the northern lake drained, followed closely by the southern lake (Figure 4.2) (Kochtitzky et al., 2020). This drainage appears to have been subglacial, close to where the ice canyon formed during the drainage in 1998. This channel closed off in the winter of 2006-2007, and both the southern and northern lakes began to reform. The northern lake drained before the end of the summer, but the southern lake persisted until the summer of 2008, when the lake finally drained, and the river rerouted along the front of the terminus of the glacier. By the time the next surge event began, in 2012, the glacier had retreated an average of 444 m since the start of the quiescent phase in 2002, but up to 650 m in some areas.

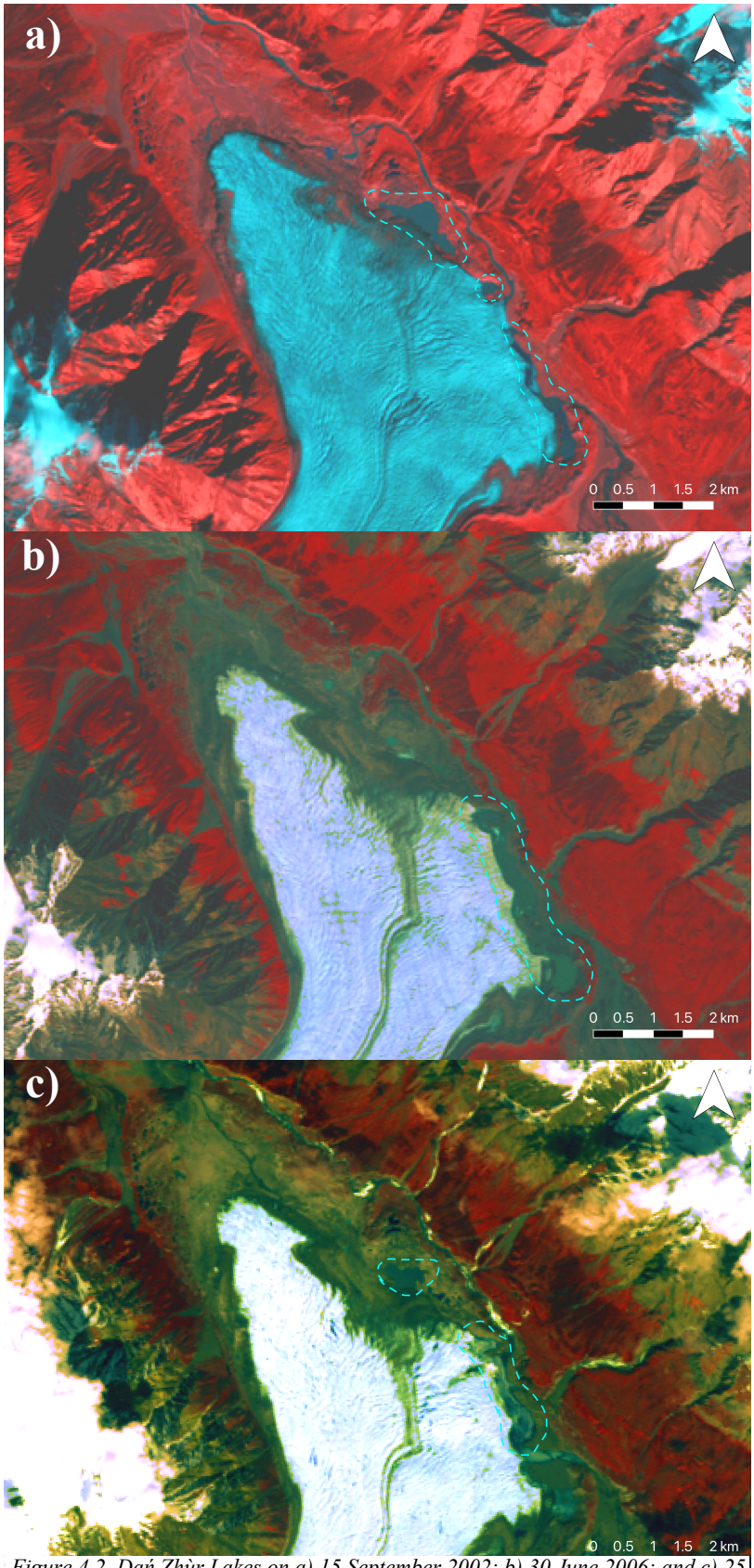

Figure 4.2. Dań Zhùr Lakes on a) 15 September 2002; b) 30 June 2006; and c) 25 May 2007 (Landsat 5 & 7). Blue dashed lines represent area where there is a lake present.

4.3 Drainage events since 2012-2014 surge

The 2012-2014 surge again dammed the Dań Zhùr Chù when the glacier front advanced by an average of 303 m and maximum of 576 m, leading to the formation of lakes beginning in the winter of 2012-2013. These lakes were able to reach a total area of 1.67 km^2 by the end of the 2013 melt season (Figure 4.3) and connected to form one lake in the summer of 2016 (Kochtitzky et al., 2020). This lake persisted until 2017, when the first rapid drainage of this quiescent phase occurred.

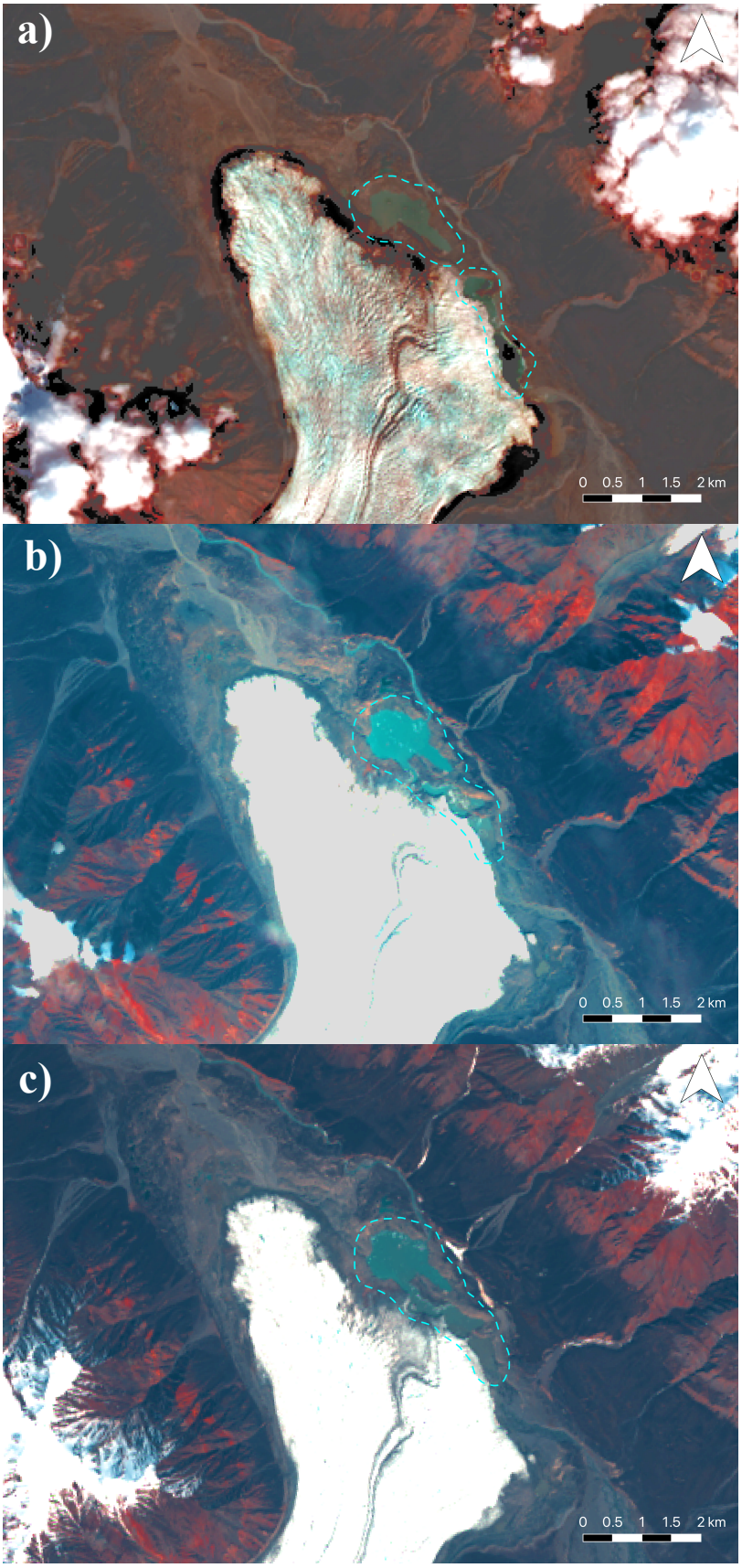

Figure 4.3. Dań Zhùr Lakes on a) 27 August 2013; b) 21 August 2016; and c) 5 June 2017 (Landsat 8). Blue dashed lines represent area where there is a lake present.

4.3.1 2017

The 2017 drainage of Dań Zhùr Lake was only partial, which can be seen in the before and after satellite imagery from August 7th, and October 10th, 2017 (Figure 4.4 a & c). The rapid drainage occurred between August 15th and 16th, 2017. The lake drained subglacially through the horseshoe-shaped outlet at the south side of the lake (red box in Figure 4.4 a), with this water flowing out of the northwest side of the terminus. The zoomed-in figure of this area for these same dates (August 7th and October 10th, 2017; Figure 4.5 a & c, respectively) shows only very minimal cracking on the ice surface where the water drained, compared to the more extensive cracking in 2018, shown in Figure 4.5 b & d.

Another important feature to note is the large volume of icebergs that can be observed on the north-east side of the lakebed (Figure 4.4 c), where free floating ice was drawn towards a drainage outlet and then became grounded on the lakebed. We can see in the before drainage image from August 7th, 2017 (Figure 4.4 a), that this area is a slow drainage outlet when the lake is full.

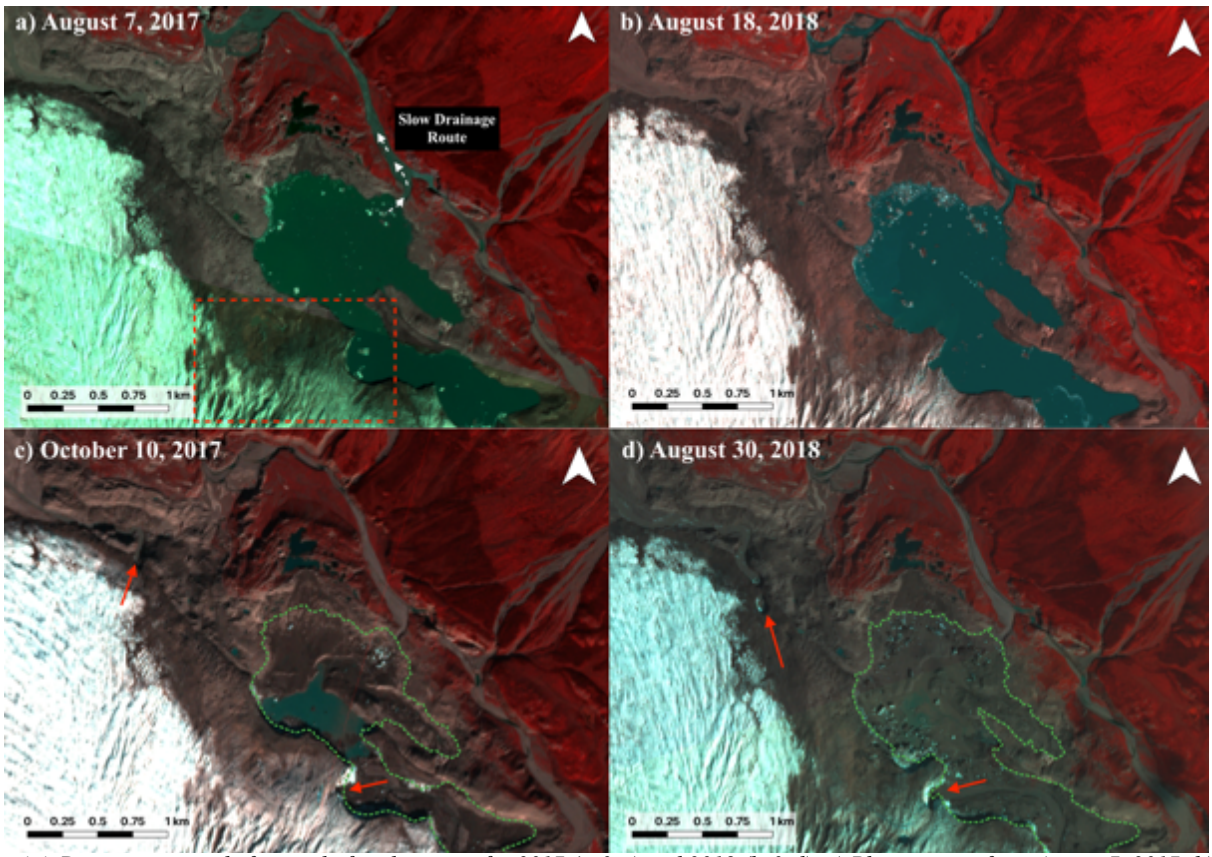

Figure 4.4. Drainage routes before and after drainage, for 2017 (a & c) and 2018 (b & d). a) Planet image from August 7, 2017; b) Planet image from August 18, 2018; c) Planet image from October 10, 2017; and d) Planet image from August 30, 2018. Green dashed line is full lake for the respective year, and red arrows are inlet and outlet of subglacial channel. Red dashed box in image a) is the extent of images in Figure 4.5.

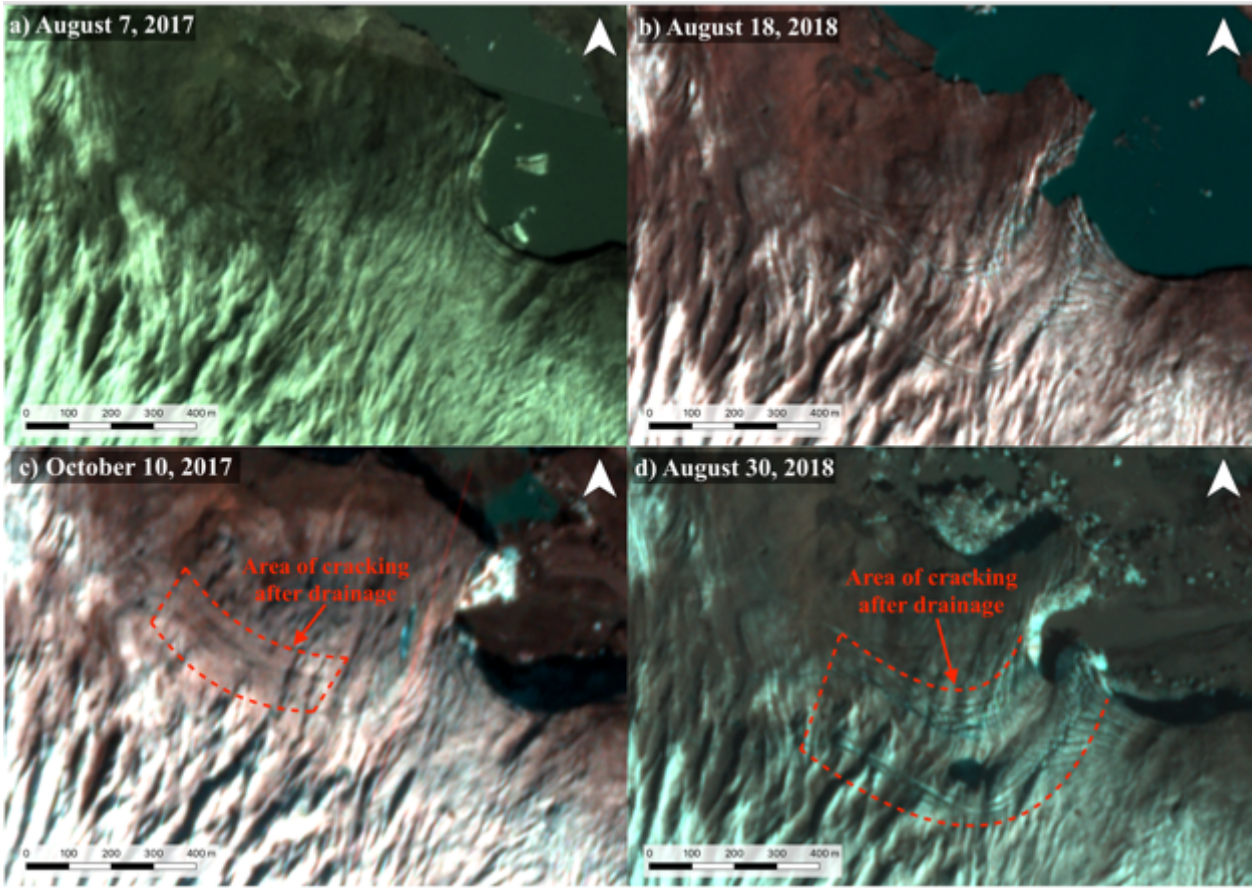

Figure 4.5 Close up (extent shown by red dotted box in Figure 4.4 a) of drainage routes before and after drainage, for 2017 (a & c) and 2018 (b & d). a) Planet image from August 7, 2017; b) Planet image from August 18, 2018; c) Planet image from October 10, 2017; and d) Planet image from August 30, 2018. Red dashed arrows in d) are the route of the subglacial channel, and significant cracking can be seen on either side of the channel.

4.3.2 2018

In 2018 we see a similar pattern to the drainage of 2017. In the before-drainage image (Figure 4.4 b) the lake appears to still be draining slowly though the river outlet at the NE side of the lake. The rapid drainage of the lake occurred between August 18th and 21st, 2018, under the terminus of the glacier, through the same subglacial channel as in 2017. In a satellite image of the lake post-drainage, we can see where the river enters the subglacial channel and drains out at the north end of the terminus (red arrows in Figure 4.4 d). In the smaller scale before image (Figure 4.5 b), we can see some crevassing on the surface of the glacier where the water eventually drains, and some of this channel collapses at both the inlet and the outlet of the subglacial channel by August 23rd, 2018, less than a week after the drainage event.

Prior to drainage, there were two large crevasses on either side of the subglacial channel in a southwest and northwest direction. The southern crevasse extended for a horizontal distance of ~835 m and the northern one ~660 m. Post-drainage the shape and direction of the crevasses were the same, but the southern crevasse was longer by almost 100 m. To the north a new crevasse developed, extending as far as 666 m in the same direction as the previous northern crevasse.

4.3.3 2019

The 2019 drainage event was captured by the two time-lapse cameras positioned facing the terminus of the glacier, which provide a detailed timeline of lake levels from July 12th, 2019, onwards (Figure 4.6). The drainage of the lake started at 17:30 local time on that date, as determined by the pressure sensor (Figure 4.7), and continued until about noon on July 15th, 2019, as determined by the time lapse cameras given that the pressure transducer was not located at the base of the lake and only recorded active drainage until 09:30 on July 13th, 2019.

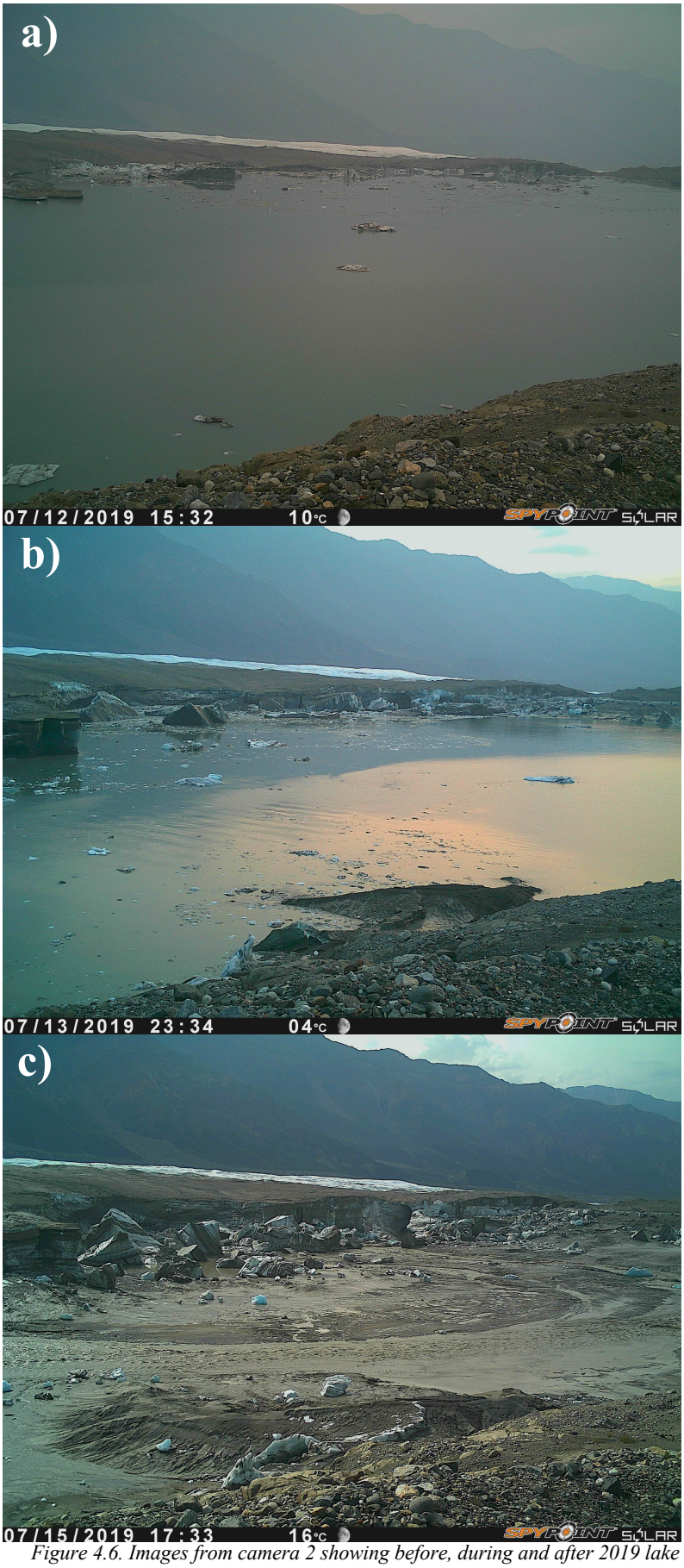

Figure 4.6. Images from camera 2 showing before, during and after 2019 lake drainage; a) 07/12/2019 15:32; b) 07/13/2019 23:34 and c) 07/15/2019 17:33.

The pressure logger shows that after the lake began to drain around 17:30 on July 12th, the lowering rate was initially gradual at below -0.10 m/h, until 23:30, when the lake began to drain faster. The lowering rate continued to accelerate until it reached -1.39 m/h at about 07:00 on July 13th (Figure 4.7). At this time there was a peak in the rate of change from 07:00 until 08:30, when the rate of lake drainage slowed, and then accelerated rapidly until it reached a rate of change of -1.76 m/h at 09:30. After this, the pressure logger was exposed to the atmosphere and no more useful data were recorded, as the water level dropped below the device.

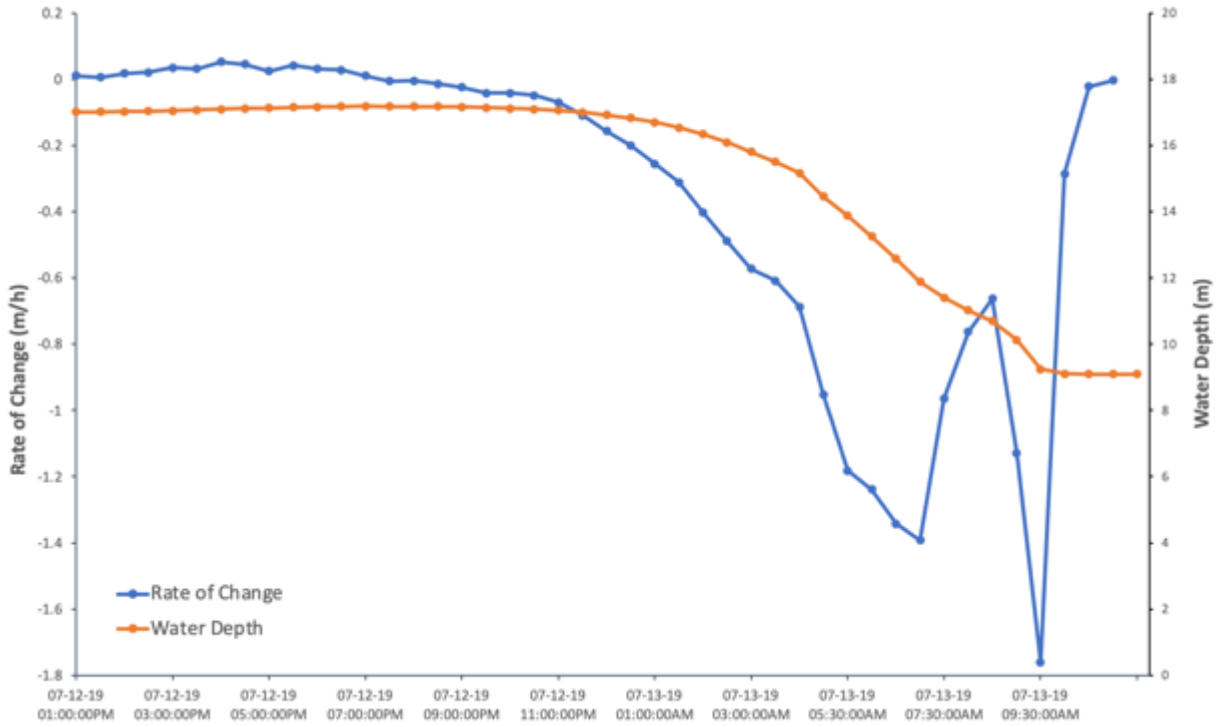

Figure 4.7. Pressure transducer record showing rate of change in m/h and lake depth in m of Dań Zhùr Lake level on July 12 and 13, 2019.

The pattern of the 2019 drainage differed from that of 2017 and 2018. Although the prominent subglacial channel where the previous two drainage events occurred is visible in the satellite imagery (Figure 4.8 a), the water did not drain through the same route in 2019. Instead, a new channel developed in the ice at the north end of the lake, very close to the boundary between the terminus and adjacent bedrock. The channel first developed subglacially and then eventually the roof collapsed to form an ice canyon through the terminus of the glacier. This new channel

cut through the terminus to connect with the downstream portion of the old drainage channel (Figure 4.8 b).

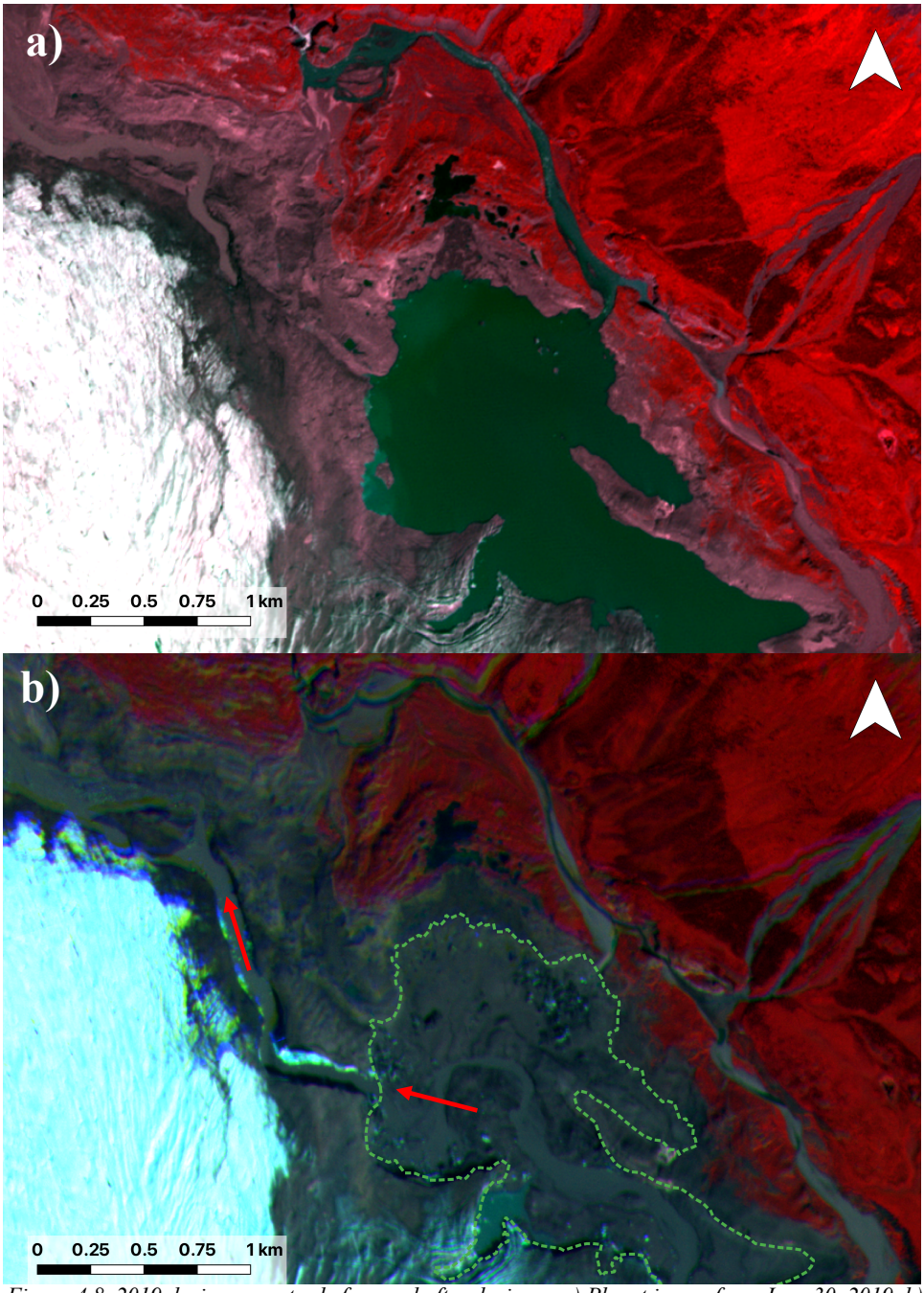

Figure 4.8. 2019 drainage routes before and after drainage a) Planet image from June 30, 2019, b) Planet image from July 26, 2019. Green dashed line is full lake from June 30, 2019, and arrows indicate ice canyon where lake drained.

Figure 4.9 shows the formation of the ice canyon after the 2019 drainage as seen in the satellite imagery. The lake drainage occurred on July 13th, 2019, but the roof of the channel didn't collapse until sometime between July 18th and July 26th, 2019. In the satellite image of July 16th, the channel was intact, other than a slight increase in size of the channel flowing out of the glacier terminus. On July 18th, some collapse of the channel roof occurred, as crevasses can be seen on either side of it, as well as a small hole that developed in between the cracking. By July 26th there was a full ice canyon through the terminus of the glacier. In the time-lapse camera images, we can see the canyon collapse from a different angle. These data show a gradual collapse after the lake has drained, until July 23rd, when the roof of the canyon completely collapsed (Figure 4.10). An illustration of the steps of how this collapse occurred is shown in Figure 4.11.

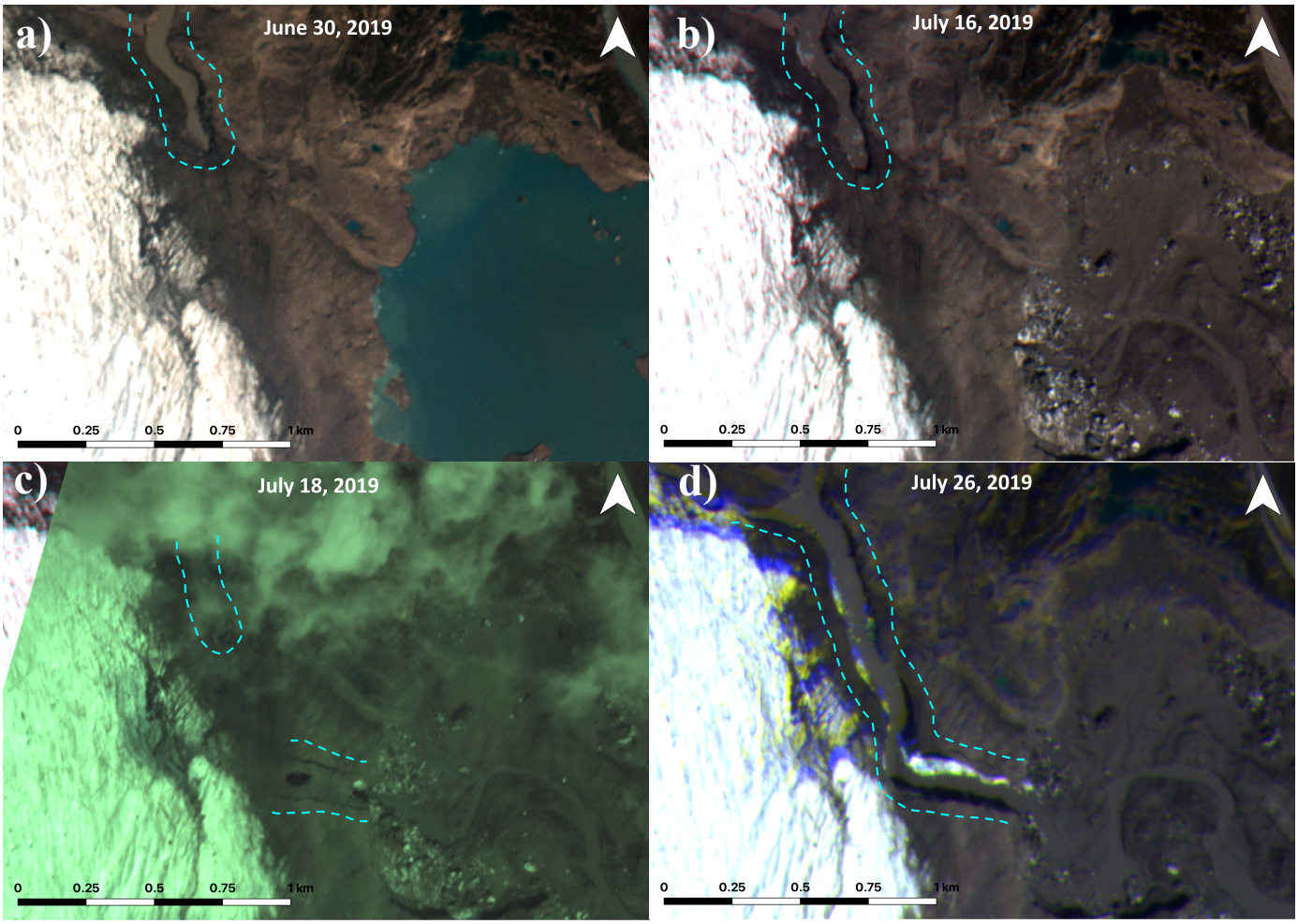

Figure 4.9. Formation of ice canyon for a) June 30, 2019; b) July 16, 2019; c) July 18, 2019, and d) July 26, 2019. Images sourced from Planet for indicated dates.

Figure 4.10. Images from camera 2 of canyon formation post drainage. Red box is region of canyon.

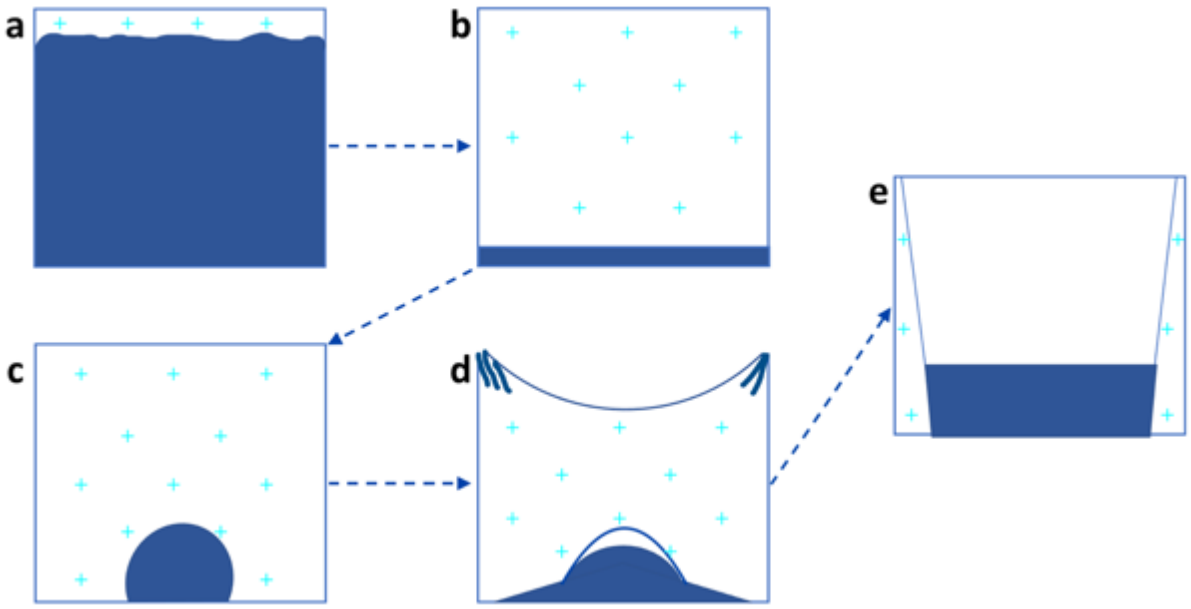

Figure 4.11. Illustration of the process of the formation of ice canyon. a) Lake is full and reaches 91.7% of the thickness of the terminus; b) flotation occurs, and water flows between ice and ground; c) water under pressure begins to carve out subglacial channel; d) continued flow of water begins to carve out the sides of the channels, the roof begins to thin from underneath and begins to cave in from the top; e) the roof fully collapses, developing into an ice canyon, through which the river drains. Areas with blue crosses represent ice.

Figure 4.12 provides two images taken from a helicopter on September 5th, 2019, flying just above the ice canyon. The image shows a subglacial drainage route demonstrated by the turbid water outflow, which is likely the old drainage channel from 2017 and 2018 connecting with the new ice canyon.

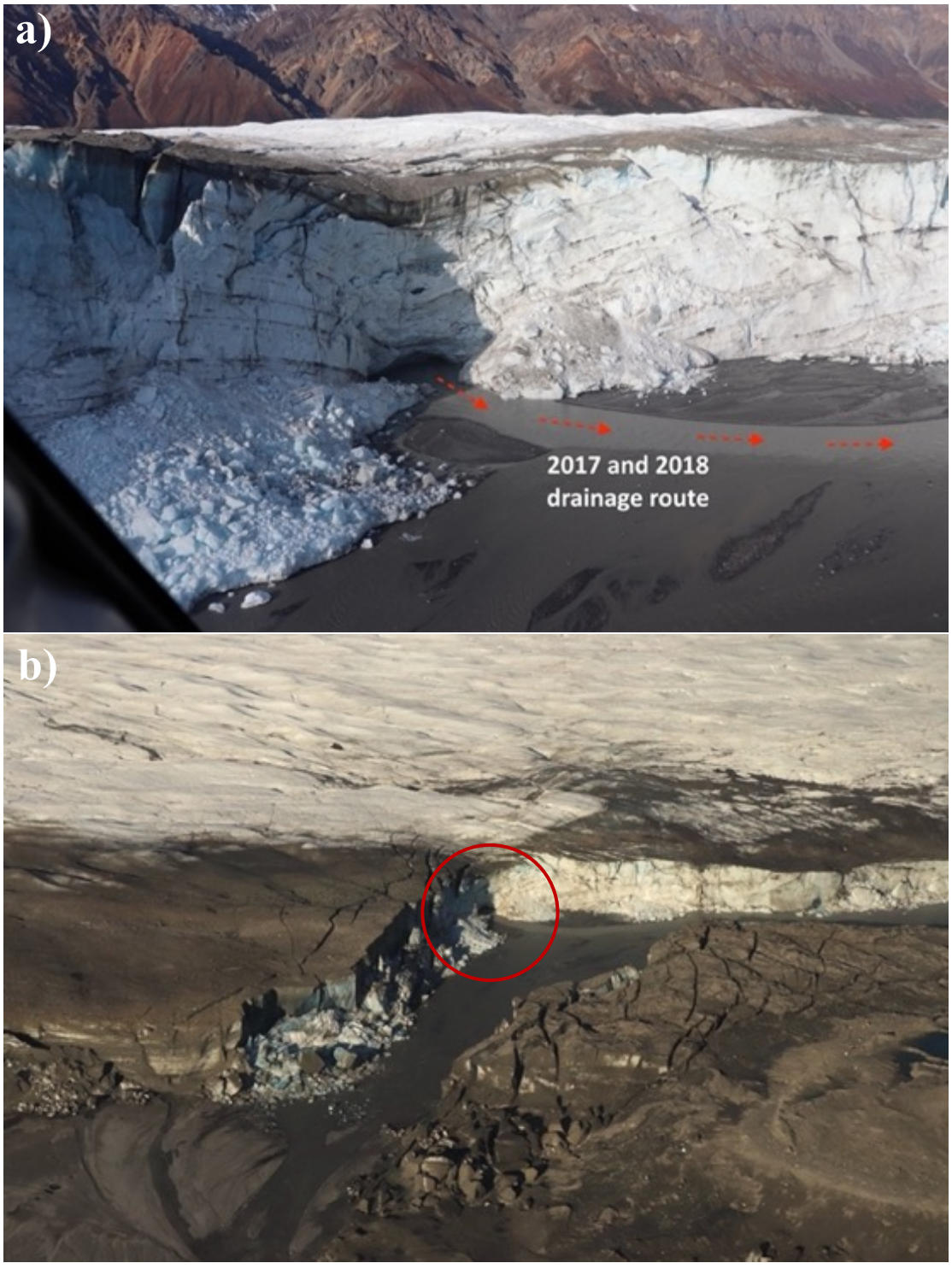

Figure 4.12. Photos from September 5, 2019, showing old subglacial drainage route connecting to the new ice canyon. Image b shows the location of the old drainage route within the ice canyon.

Figure 4.13 provides an illustration of the likelihood of flotation at the terminus of the Dań Zhùr Glacier when the lake was at its maximum in July of 2019. The red areas are most likely to float, and the blue areas least likely to float, calculated using the measured thickness of the ice and depth of the lake derived from 2019 airborne DEMs, as well as the densities of both ice and water. At the terminus of the glacier, there are two areas that stand out as most likely to float. These areas are the southwest corner of the lake, where the canyon eventually formed, and to the east of the drainage outlet from 2017 and 2018.

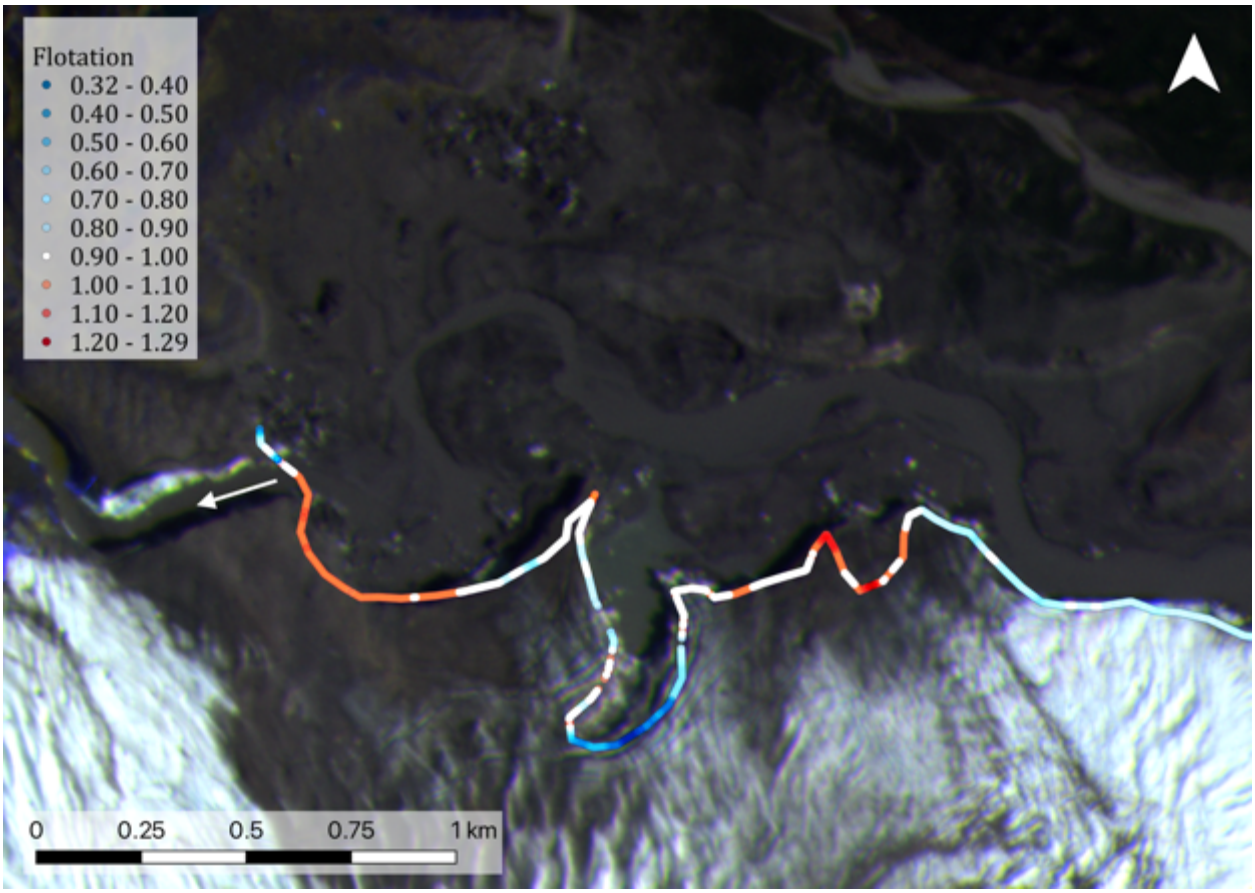

Figure 4.13. Regions of flotation, relative to a full 2019 lake, at the terminus of Dań Zhùr. Areas in red are very likely to float (> 1), and areas in blue or white are unlikely to float (< 1), based on the difference in height derived from the DEMs. White arrow indicates area where canyon formed in 2019.

In order to determine how much the glacier thinned over the summer of 2019, the surface melt rate at the terminus of Dań Zhùr Glacier was calculated using a time-lapse camera and a striped pole drilled into the ice surface. The average melt rate between July 12th, 2019, and August 6th, 2019, was 5.5 cm of vertical ice loss per day. This can also be inferred from the melt

rate near the terminus of the Kaskawulsh Glacier, which sits at a similar elevation to the Dań Zhùr Glacier. Between 2007 and 2018 the lower ablation area of Kaskawulsh Glacier thinned at an average rate of >2 m a^{-1} (Young et al., 2021).

4.3.4 Lake area and volume changes

Lake area and volume, calculated using high-resolution DEMs and satellite imagery, are presented in Table 4.1 and Figure 4.14 for July 7th, 2017, August 18th, 2018, and July 6th, 2019, when the lake was close to its annual maximum extent, just prior to drainage. Both the volume and area of Dań Zhùr Lake increased in size each year between 2017 and 2019, with the increase greater between 2018 and 2019, as illustrated by the slight steepening of the slope of the graph in Figure 4.14. Between 2017 and 2018, the lake area grew by 0.41 km^2, and the volume by 0.00887 km^3, and between 2018 and 2019 the area of the lake grew by 0.55 km^2, while the volume increased by 0.01473 km^3.

Table 4.1. Area and volume of Dań Zhùr Lake in 2017, 2018 and 2019.

Date (dd/mm/yyyy)	Area (km^2)	Volume (km^3)
07/07/2017	1.49	0.01657
18/08/2018	1.90	0.02544
06/07/2019	2.45	0.04017

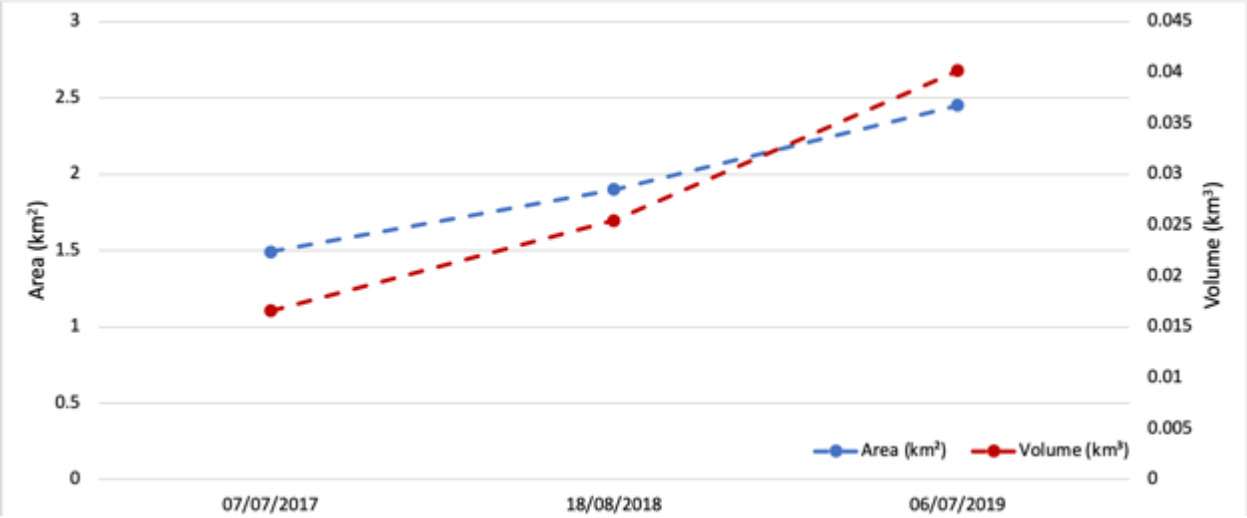

Figure 4.14. Area and volume of Dań Zhùr Lake in 2017, 2018 and 2019. Points represent volume and area of lake in during each year.

4.4 Long term changes in terminus position

At Dań Zhùr Glacier there has been a trend of long-term terminus retreat over the past three surge cycles. Each surge since 1990 has reached a lesser maximum extent than the previous surge (Figure 4.15), consistent with retreat driven by a warming climate. The 1990 surge extended an average of 377 m past the 1988 limit, and a maximum of 775 m in one area of the terminus, further than the 2014 surge (Figure 4.16). The difference in surge extents is more prominent near the middle and north end of the terminus than at the south end of the terminus.

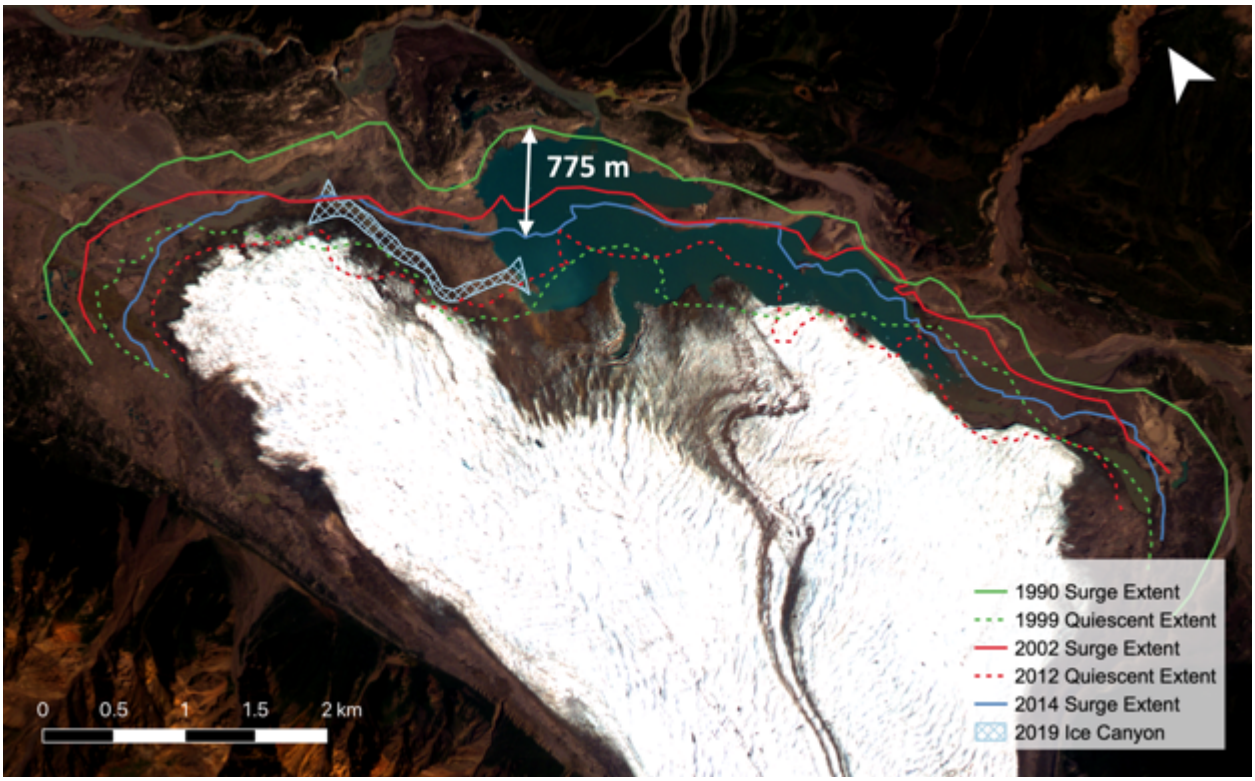

Figure 4.15. Surge and quiescent terminus extents for the last three surge cycles (Planet image from June 30, 2019). White arrow is the distance retreated from the 1990 surge extent to the 2014 surge extent.

Within a single surge cycle, we can also see the terminus retreat that occurred between 2017 and 2019 during a quiescent period (Figure 4.16). The most significant retreat over these years is at the northwest end of the lake, near the 2019 drainage route, where the ice front retreated 326 m between 2017 and 2019. This is more than 2.5 times the retreat that occurred closer to the middle and south side of the terminus (Figure 4.16).

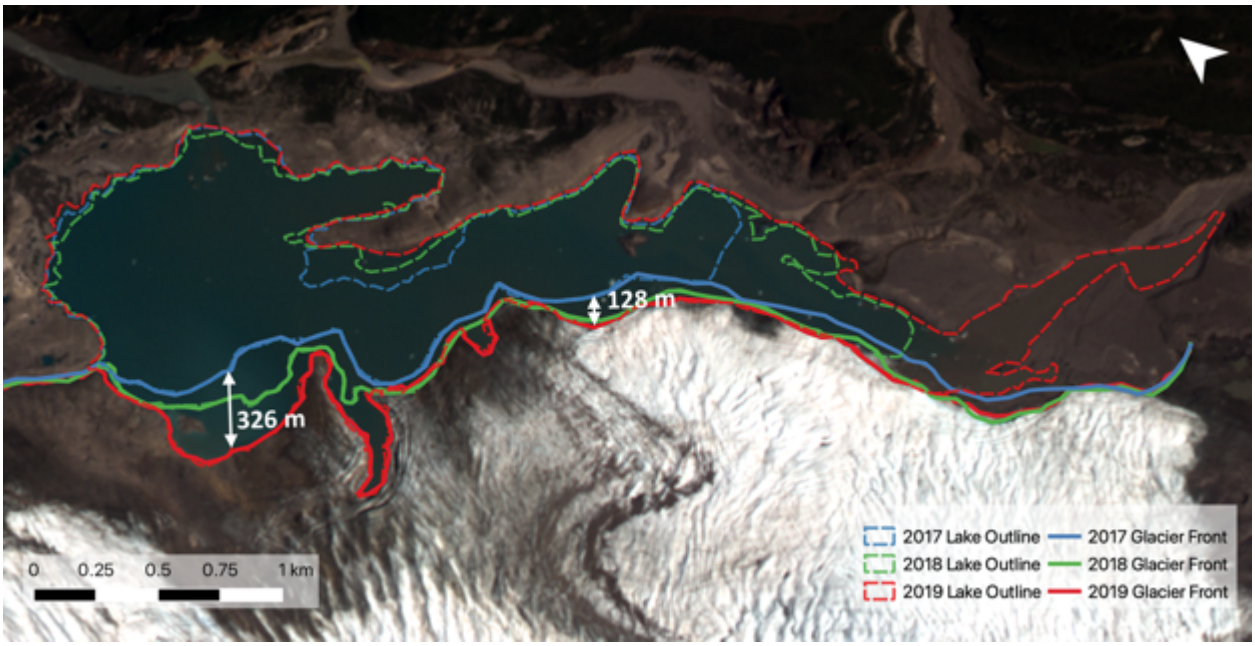

Figure 4.16. Lake extent and terminus positions for 2017, 2018 and 2019 (Planet image from June 30, 2019).

4.5 Summary

This chapter presented the results of the causes, patterns, and mechanisms of the drainage of Dań Zhùr Lake over the last three surge cycles since 1988-1990. With each surge cycle there is a trend of increasing lake size and volume, particularly in 2017, 2018 and 2019. The following chapter discusses the implications of a larger Dań Zhùr Lake, and what hazards might be posed by these lake drainage events in the SW Yukon.

5.0 Discussion

Recent lake drainage events at Dań Zhùr Glacier, including the 2019 GLOF, have occurred due to the formation of both glacier-dammed and moraine-dammed lakes, controlled by flotation and glacier dynamics. Dań Zhùr Lake is a proglacial lake that forms when the Dań Zhùr Glacier surges and advances far enough into the valley to block the flow of the Dań Zhùr Chù'. This is a phenomenon that has been seen in other locations around the world, such as the Karakoram, Pamirs, Andes, and in Alaska (Bazai et al., 2020; Round et al., 2017; Harrison et al., 2015). In many of these cases, the damming of water bodies due to surging resulted in GLOF events, through many different mechanisms (Harrison et al., 2015). The 2019 GLOF at Dań Zhùr Glacier was triggered by flotation of the terminus, which is a mechanism that has been previously observed by Carrivick et al. (2017) at Russell Glacier, Greenland.

In this chapter the events of both historical and more recent GLOFs at Dań Zhùr Glacier are put into the larger context by comparing them to other events around the world. Changes in glacier extent are also compared to changes in lake size and drainage patterns over the past three surge cycles, followed by discussion of the downstream risks that may arise from the rapid drainage of lakes at the terminus of the Dań Zhùr Glacier.

5.1 Timing of Dań Zhùr Lake drainage events

The quiescent phases following the 1988-1990 and 2012-2014 surges both had three lake drainage events, while four drainages occurred after the 2000-2002 surge (Figure 5.1). During each quiescent phase there were times when the lake fully drained, as well as times when the lake only partially drained, although the period between each surge and subsequent drainages did not stay constant over time. Since the 1988-1990 surge event, lakes typically form in the early winter and drain in the late summer. The patterns were as follows:

(a) The drainage events after the 1988-1990 surge occurred twice in 1997 and once in 1998, close to the end of the quiescent phase. The first two drainages in 1997 were only partial, while the one in 1998 drained the lake completely. Between the end of June and middle of August 1997, the northern lake drained into the southern lake, reducing the total lake area from 1.1 km^2 to 0.9 km^2. In the fall of 1997, another partial drainage occurred, reducing the total lake area to 0.32 km^2. The final drainage of this surge cycle, in the spring of 1998, fully drained the remainder of the lakes.

(b) The drainage events after the 2000-2002 surge occurred further in time apart from each other than in the previous cycle, and nearer to the beginning and middle of the quiescent phase. The first drainage occurred in 2001, when the lake was displaced by the advancing terminus as the glacier continued to surge. The second two drainage events occurred in 2006, when the northern lake drained first, leaving behind only the southern lake, which drained shortly after. The first of these two events occurred at the end of June 2006, when the lake area reduced from 1.12 km^2 to 0.76 km^2. The second drainage happened within a month after the previous drainage, fully emptying the remaining southern lake. The final drainage of this surge cycle was a full drainage, which happened in mid-summer of 2008, three years before the next surge would begin.

(c) The most recent drainage events all occurred in subsequent years, about 3-5 years after the most recent surge in 2012-2014. The drainage in 2017 was only a partial drainage, while those in 2018 and 2019 were full drainages. The 2017 drainage occurred between August 15th and 16th, when the 1.49 km^2 lake mostly drained, leaving behind about 0.37 km^2. Between August 18th and 21st, 2018, there was a full drainage of the lake that had reformed since 2017, which had reached about 1.9 km^2. The most recent drainage was a full drainage of the 2.45 km^2 lake, on July 12th, 2019.

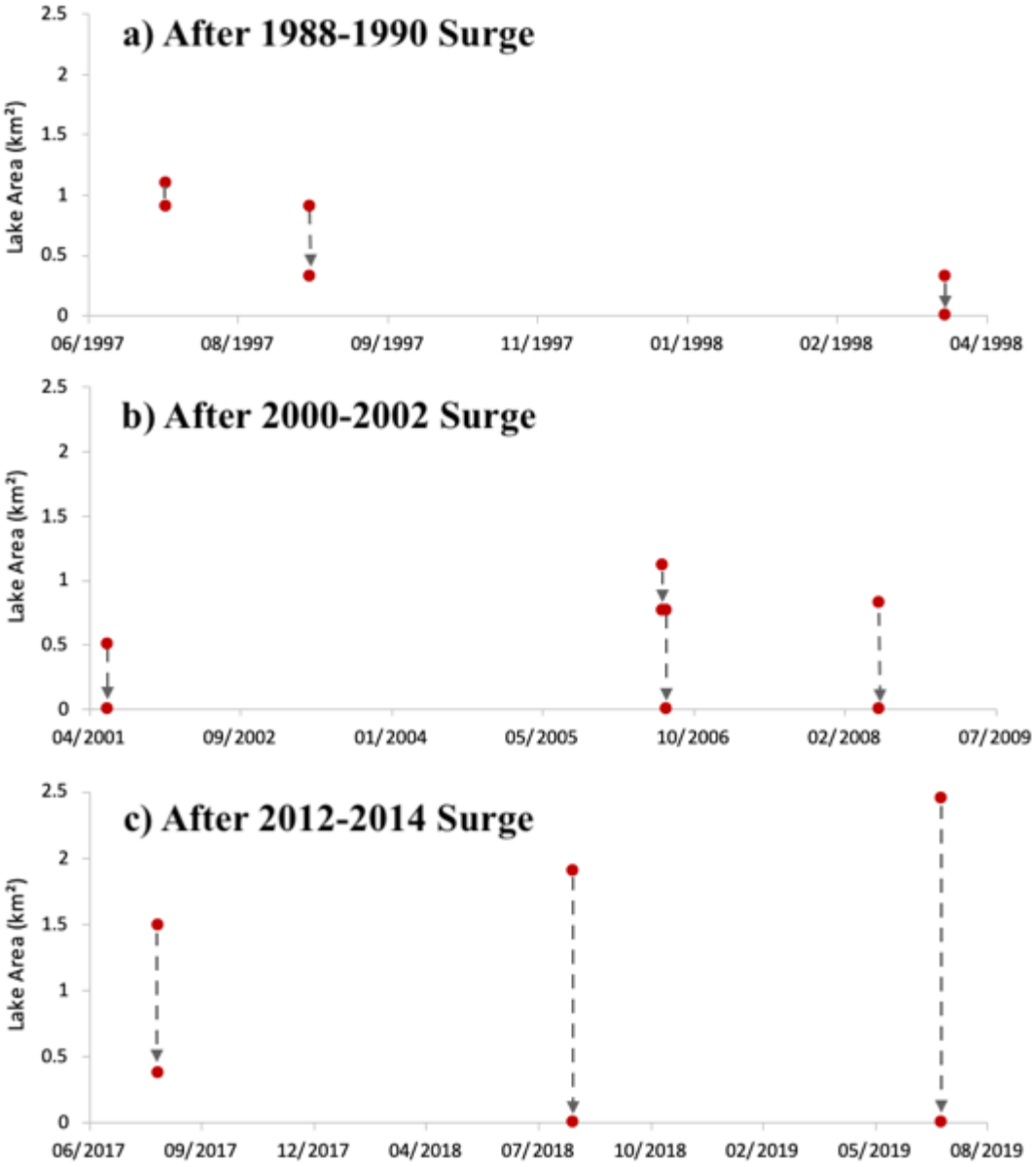

Figure 5.1. Change in lake area of each drainage event during the quiescent phase that followed the a) 1988-1990, b) 2000-2002 and c) 2012-2014 surge events of Dań Zhùr Glacier.

5.2 Mechanism of Dań Zhùr Lake drainage events

Although there is no clear pattern of when the drainage events happen after a surge, there appear to be some similarities between the mechanisms of drainage during each different period. All the drainage events occurred subglacially (i.e., through a channel under the terminus of the glacier), however after the final drainage of each surge cycle the subglacial channel collapsed to form a canyon, while during the first two or three drainage events the roof of the channel remained intact. Between the end of June and middle of August 1997, the northern lake drained into the southern lake, and then in the fall of 1997 the lake drained beneath the glacier but did not cause collapse of a subglacial channel to form an ice canyon. The first lake drainage of the following cycle, in 2001, occurred due to glacier advance, and the following two, between June and August of 2006, occurred when both the northern and southern lakes drained subglacially. The first two drainage events that occurred during the most recent surge cycle, in 2017 and 2018, also both drained subglacially. Although these lakes all drained under the glacier, each advance of the terminus during a new surge event must have altered the subglacial drainage system and shut down previous channels, so for the most part the lakes drain through different channels over different surge cycles.

Formation of the ice canyon in the final drainage of the surge cycle occurred in 1998 when the lakes drained as the Dań Zhùr Chù' flowed underneath the terminus of the glacier that spring (Figure 5.2). The roof of the channel partially collapsed within a couple of months after the drainage, and by September 1998 the entire ~4 km long and ~100 m wide roof of the channel collapsed. Similarly, in 2008, the lake drained as the river routed past the terminus. This time the river flowed primarily in front of the ice, but there was a portion of the route that was subglacial, about 1.8 km long and 150 m wide, which eventually collapsed. Finally, in 2019, the lake drained subglacially through a channel under the northeast lobe of the terminus, which collapsed ~10 days later, again forming a large ice canyon, about 2.5 km long and 100 m wide, through which the Dań Zhùr Chù' continues to drain at present (summer 2021). In each of these cases, the collapse of the roof of these subglacial channels and formation of an ice canyon prevents a lake from forming again until a new surge begins, as the canyon continues to expand from surface melt and river erosion in the years following formation (Figure 5.3). In the case of the most recent canyon: on September 9th, 2019, the channel was 175 m wide; on July 16th, 2020, it was 252 m wide and by July 9th, 2021, the ice was nearly gone on the north side of the canyon,

with only a small amount of dead ice remaining (Figure 5.3 and Figure 5.4). During a surge there is sufficient deformation of the ice to close the ice canyon or subglacial channels over a matter of months. The maximum velocity of the terminus of Dań Zhùr Glacier during the 2012-2014 surge event was 1150 m/year (Kochtitzky et al., 2019), so based on the average ice canyon width of 220 m from the past 3 quiescent phases, it would have taken approximately 2.3 months for the canyon to close once the next surge began.

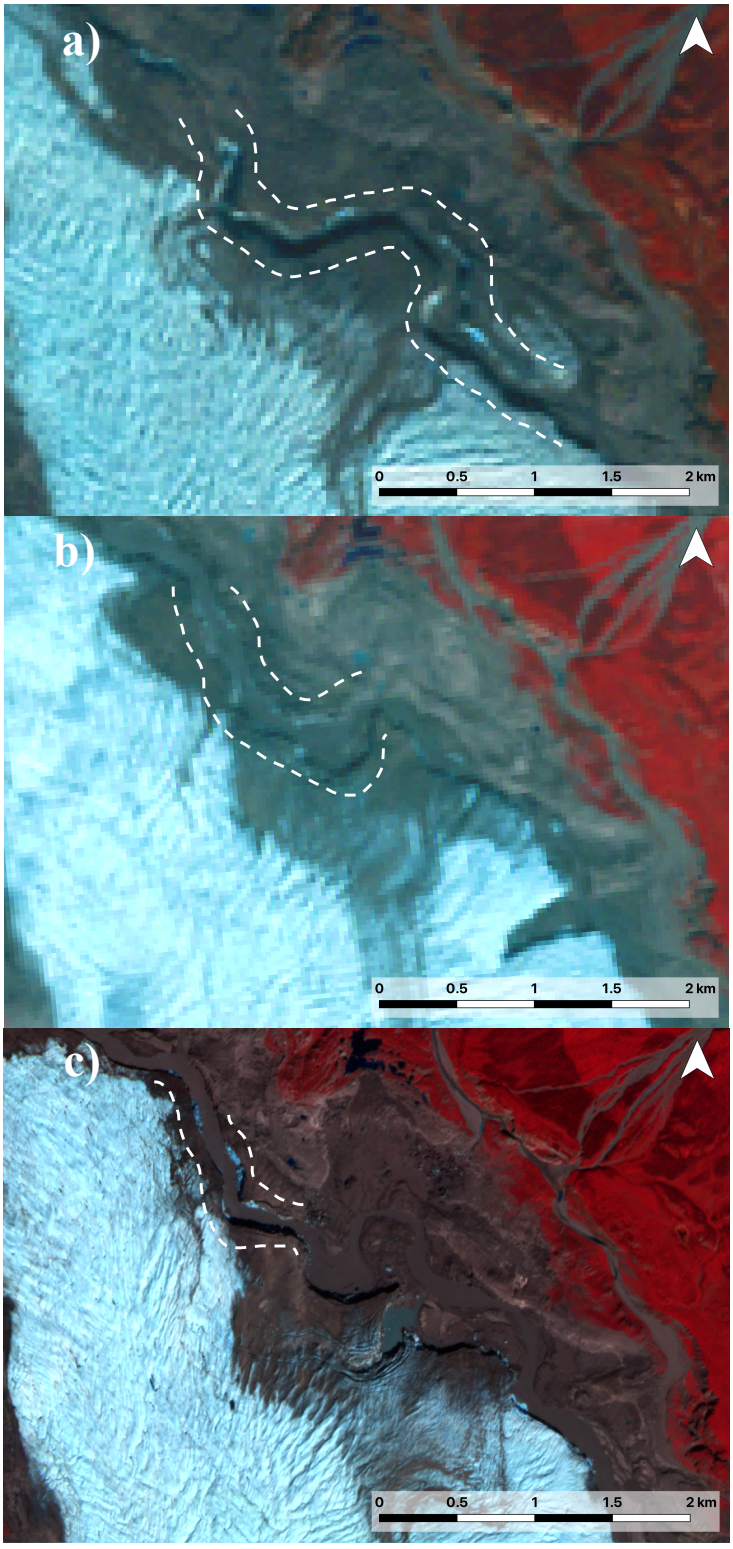

Figure 5.2. Lake drainage routes in a) September 28th, 1998; b) August 15th, 2008; and c) August 4th, 2019. Images a) and b) are Landsat 5 sourced from the USGS Earth Explorer and image c) is a Planet image sourced from the Planet website.

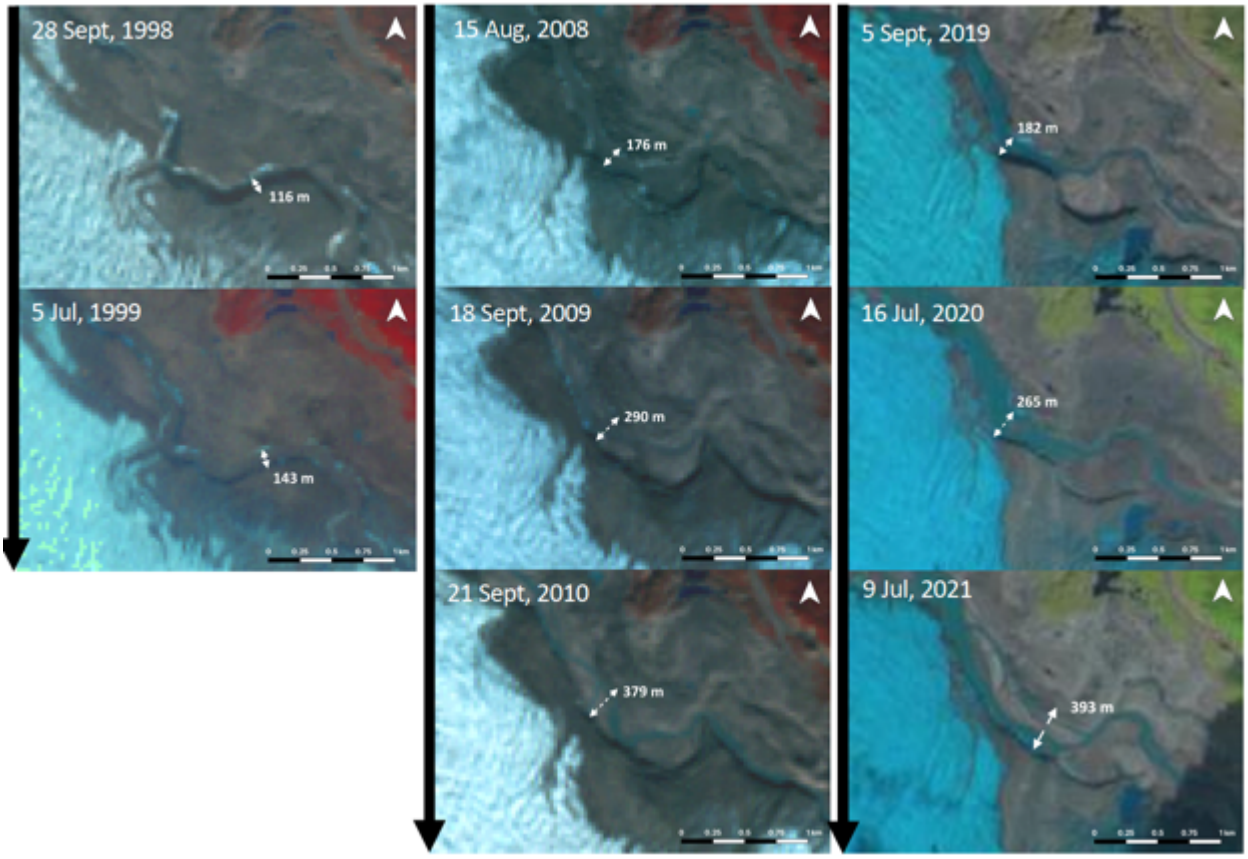

Figure 5.3. Expansion of ice canyon for two years after formation, over three different surge cycles. Images in the first column are sourced from Landsat 5, images in the second column are from Landsat 7, and images in the last column are from Sentinel 2A.

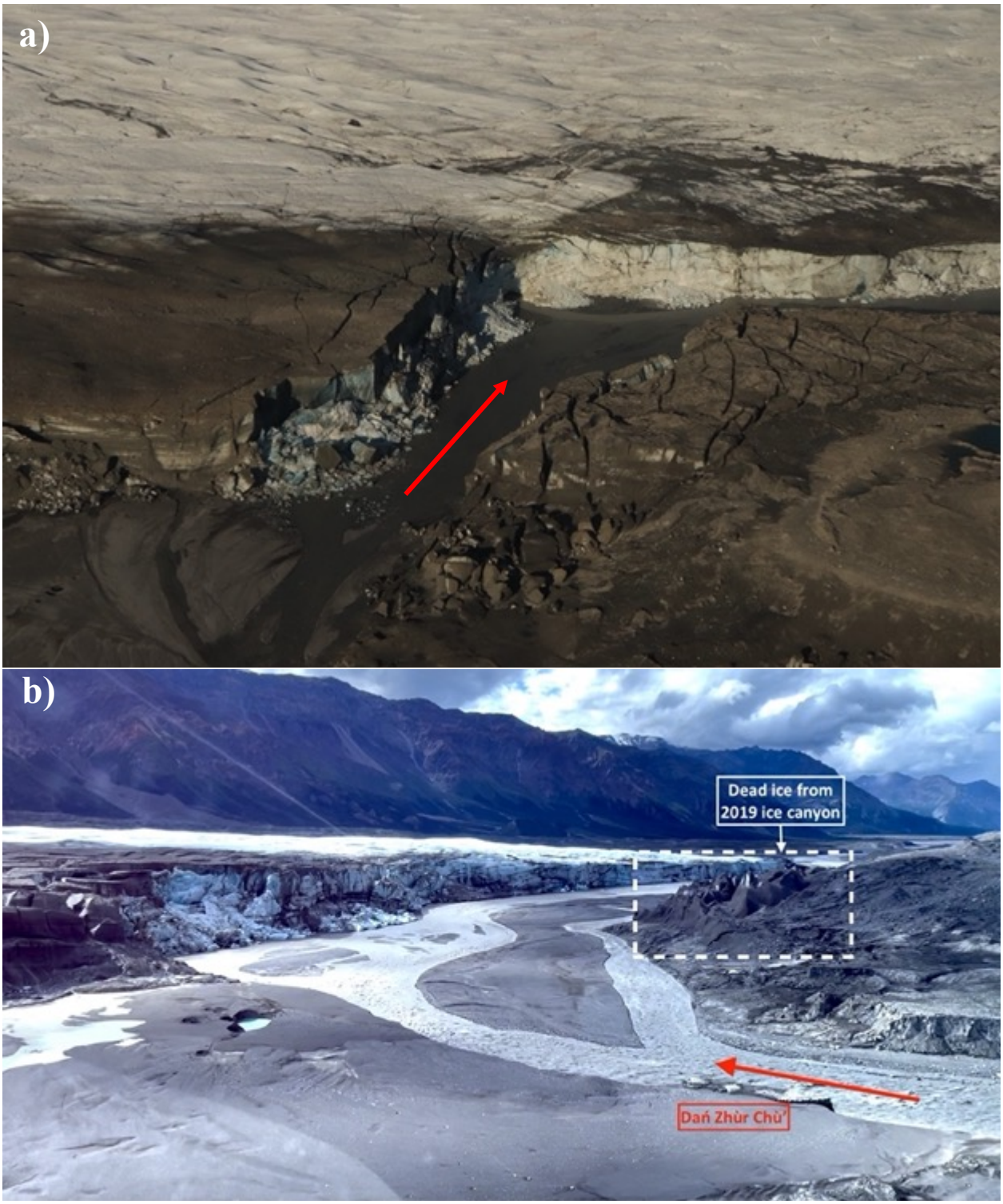

Figure 5.4. Ice canyon on September 5, 2019 (a), and ice canyon on July 27, 2021 (b). Red arrows indicate direction of river flow. Extent of a) is shown as white dotted box in Figure 5.6.

5.2.1 2017 drainage

The 2017 lake drainage was the first since the 2012-2014 surge event and was also the first time that the subglacial drainage channel formed in that part of the terminus over the past 3 surge cycles. The minimal surface crevassing above the channel in 2017, compared to later years, indicates that the subglacial channel expanded significantly between 2017, 2018 and 2019. The increased crevassing occurs as the roof of the channel subsides once the lake has drained.

The 2017 drainage was only partial, with the lake area reducing from about 1.49 km^2 to 0.37 km^2 over 2 days. It is possible that ice where the channel formed was thin enough in 2017, at an average estimated thickness of 55 m (based on the difference between the lake bed and glacier surface in the 2019 DEM, corrected for a mean annual melt rate of 5.5 m), that the terminus was able to float in that area, draining part of the lake, until there was not enough water left to maintain flotation, or establish a large subglacial channel. Once the terminus stopped floating as the lake level dropped the subglacial channel would have closed due to the weight of overlying ice, together with ice deformation, resulting in drainage from the lake being stopped. This cycle of flotation, leading to drainage of the lake, then reforming of the lake as the glacier is once again grounded, has been seen at other glaciers. For example, at the Kaskawulsh Glacier, also in the St. Elias Mountains, there was an ice-marginal lake that drained when the adjacent ice shelf reached flotation (Bigelow et al., 2020). Once the lake had drained and the ice shelf again grounded, the lake began to reform (Bigelow et al., 2020). Another example of lake drainage due to flotation is at Catalina Lake, East Greenland (Grinsted et al., 2017). Drainage events there were also cyclical, although on a longer time scale than those at the Kaskawulsh Glacier. At Catalina Lake, the lake grows until it reaches the size necessary to float the ice, drains, and then begins to refill once again (Grinsted et al., 2017). The large size of Catalina Lake means that it takes longer to refill than smaller proglacial lakes, about 10-20 years (Grinsted et al., 2017). The thinning of the glacier ice as the climate warms, however, could mean that the time that it takes for the lake to reach the depth that can float the glacier may be reduced. This is something that we could see at many different glacial lakes (Grinsted et al., 2017).

5.2.2 2018 drainage

In 2018 the lake drained through the same channel as in 2017, but this time it fully drained. In 2018 the lake was larger, at 1.9 km^2, and the passing of another melt season meant

that the ice at the terminus of the glacier would have been thinner by about 5 m, as determined by the ablation measurements. Because of these two factors, as well as the pre-established location of the channel from the previous year, the lake was able to drain completely, and enlarge the subglacial channel even more compared to 2017. There was much more significant crevassing on the surface of the glacier where the channel formed in 2018 than in 2017 (Figure 5.5). There were two main crevasses which developed on either side of the subglacial channel, about 150 m apart from each other. The northern one extended to almost a kilometer in length, and the southern one to about 670 m after the lake had drained. The larger crevasses suggest that the channel enlarged, and its roof thinned between 2017 and 2018, as water drained through it.

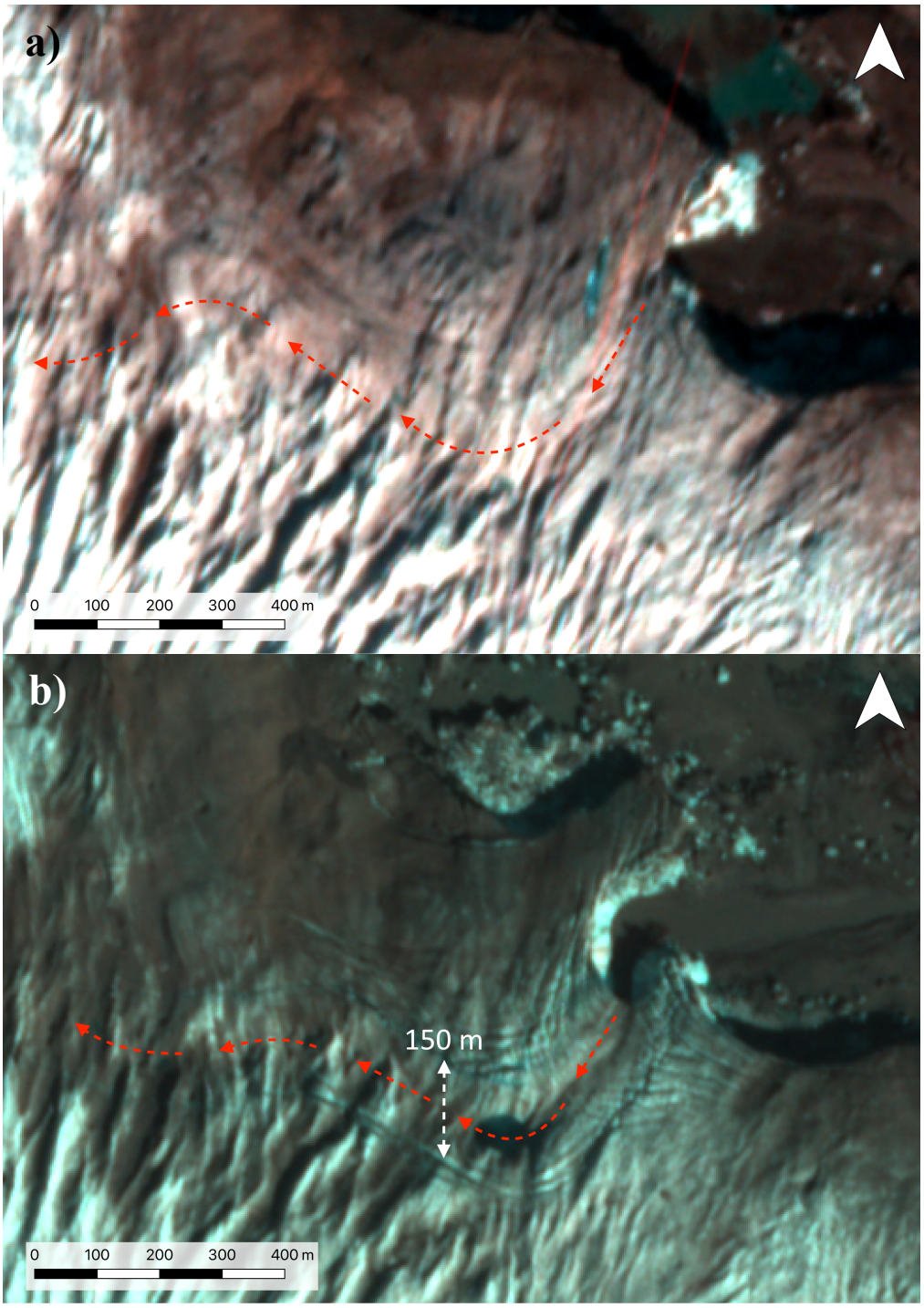

Figure 5.5. Crevassing on the surface of the terminus near the 2017/2018 drainage route. Image a) is a Planet image from October 1st, 2017, and image b) us a Planet image from August 30th, 2018. Red arrows indicate direction of river flow in subglacial channel, white arrow indicated the distance between crevasses.

5.2.3 2019 drainage

The 2019 lake drained through a subglacial channel in a different location than in 2017 and 2018. The channel formed at one of the thinnest ice areas of the terminus, and the later collapse of its roof shows that it merged with the lower part of the 2017/2018 subglacial channel (Figure 5.6). Figure 5.7 shows how the canyon grew after the drainage of the lake in 2019. The 2019 lake was the largest ever recorded (Kochtitzky et al., 2020), measuring 2.45 km^2 on July 6th, 2019. The area where the channel formed in 2019 was further north of the 2017/2018 drainage channel, closer to the northern margin of the glacier. This was one of the thinnest and lowest elevation areas along the terminus at the time of the 2019 drainage, making it the first region to float when the lake was at maximum depth. The 2019 channel also occurred in the part of the terminus with the least distance to reach the previous 2017/18 subglacial channel, only about 500 m (Figure 5.6). Once the terminus was floating, it is likely that the water began to flow underneath as a sheet, and then concentrated along the steepest hydraulic gradient, in this case the shortest distance between the area of flotation and the outlet.

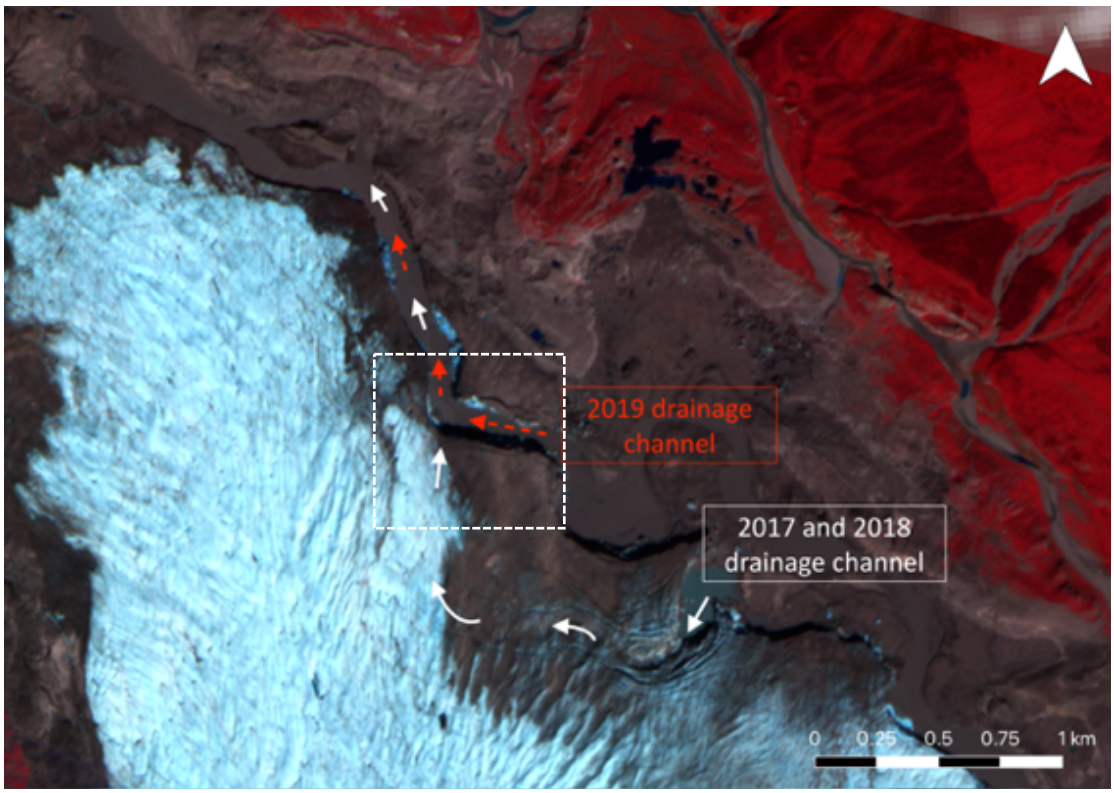

Figure 5.6. The 2019 drainage channel (red arrows) intersected the 2017/2018 drainage route (white arrows). White dotted box is extent of Figure 5.4 a).

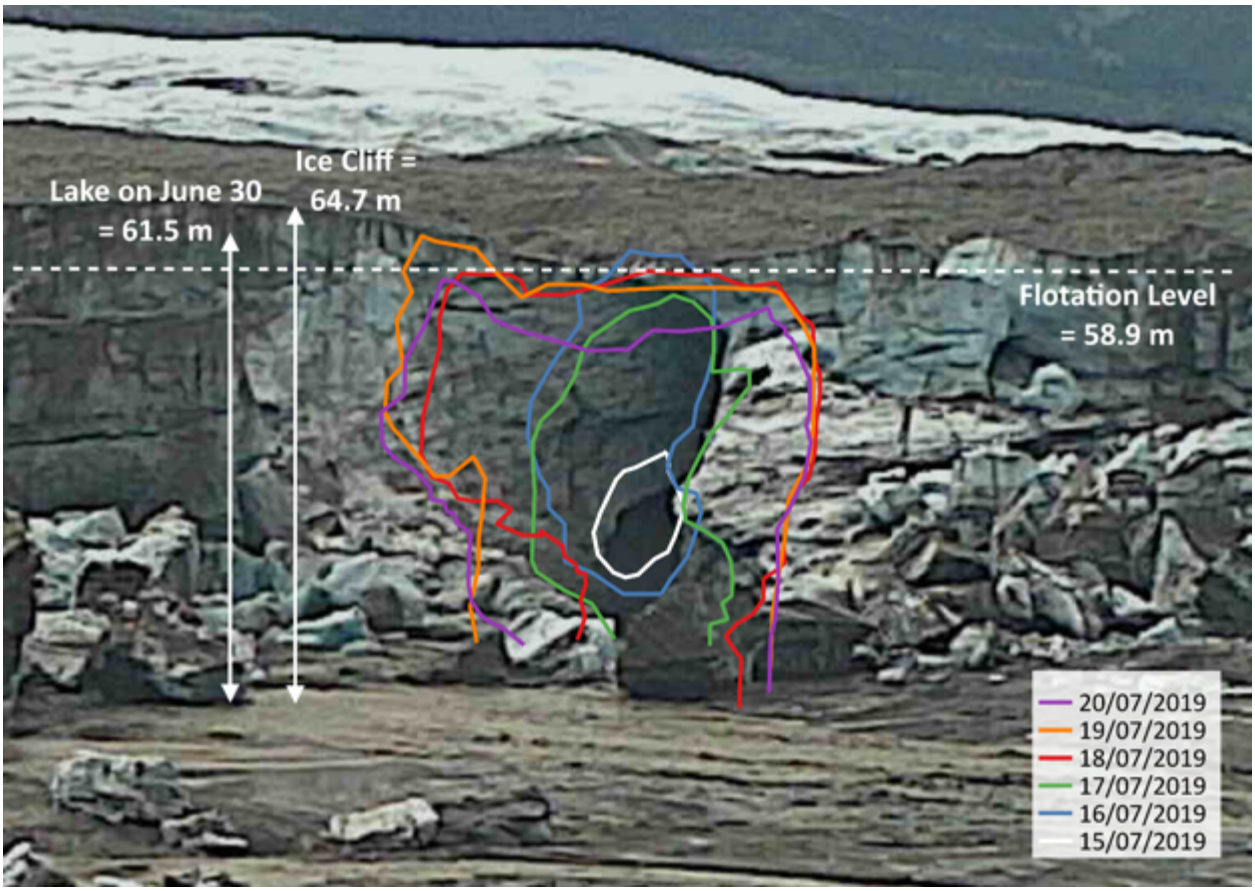

Figure 5.7. Progression of 2019 ice canyon from July 15th to July 20th, 2019. Flotation level of the terminus when the ice cliff measures 64.7 m is 58.9 m (white dotted line). The lake on June 30th, 2019, was at a 61.5 m, therefore flotation occurred.

It is also important to note that the 2017, 2018 and 2019 lakes all drained slowly out of a subaerial stream at the northeast end of the lake before the rapid subglacial drainage events (Figure 4.4a). This stream provided a consistent slow drainage of the lake that routed around part of the Neoglacial maximum moraine and joined the main Dań Zhùr Chù' about 5 km downstream. As soon as the lake reaches a surface elevation of about 1087 m above sea level, water begins to drain out of this channel, controlling the maximum height that the lake can reach. This outlet does not, however, limit the maximum area of the lake because as the glacier retreats it exposes a larger, and potentially deeper, lake basin. Due to overdeepening of the ground beneath the glacier from previous glacial cycles, the lakebed is getting larger and deeper as the glacier retreats. However, because each surge event so far has covered the lake basin, it takes some time after the surge has ended for the glacier to retreat enough to expose the basin and allow a lake to begin to form. Kochtitzky et al. (2020) found that since the 2000-2002 surge,

lakes that form at Dań Zhùr Glacier during the quiescent period after a surge have become larger in size, likely because more of the basin is exposed as the glacier terminus does not reach as far into the valley during a surge event as it did in the past.

There is also a large difference in elevation between the area where the subglacial ice canyon developed in 2019 and the secondary subaerial outlet. As previously mentioned, the secondary outlet was at an elevation of about 1087 m, while the elevation of the lakebed where the ice canyon formed in 2019 was about 1035 m, approximately 50 m lower. The lake could never fully drain out of the secondary outlet because the elevation of the lake basin is much lower than this outlet.

5.3 Implications of flooding downstream

One of the main concerns of GLOFs around the world are downstream hazards as water drains rapidly from the lake (Haeberli et al., 2015; Hock et al., 2019). Historically there have been many GLOFs that have led to significant downstream destruction. One of the most notable examples is the 1941 GLOF that occurred near the city of Huaraz, in Peru, which killed more than 6000 people and destroyed about a third of the city (Clague & Evans, 2000). Another more recent event in the Indian Himalayas saw more than 6000 fatalities from a lake outburst flood and large landslide (Allen et al., 2016). The June 2013 event in the village of Kedarnath was initiated by heavy rainfall, which caused a moraine dammed lake to fail (Allen et al., 2016). Although western North America experiences outburst floods with some of the largest volumes, they are also the events with the least amount of damage, due to relatively little infrastructure and low populations in mountainous areas (Carrivick & Tweed, 2016).

In the case of Dań Zhùr Lake, the main potential risks are to recreational users of the area and the Alaska Highway bridge that crosses the Dań Zhùr Chù' about 50 km downstream of the terminus. Modelling undertaken by Clarke and Mathews (1981) suggests that a large lake caused by a full blockage of the Dań Zhùr Glacier valley could lead to significant damage to downstream infrastructure if it were to rapidly drain. They used aerial photographs to determine the most likely point where the ice would dam the river and calculate the reservoir volume corresponding to the contour area of the empty basin and made comparisons with an outburst flood with a very similar reservoir size in Summit Lake, British Columbia, to interpret some of the lesser-known variables, like Manning roughness and lake temperature. They concluded that if

Dań Zhùr Lake were to re-form, the peak discharge would most likely be between 3968 and the 5968 $m^3 s^{-1}$, with some variation depending on tunnel outlet location (Clarke & Mathews, 1981). However, a full blockage of the valley is very unlikely to occur due to the consistent retreat of the glacier since the 1930s (Kochtitzky et al., 2019).

The area downstream of Dań Zhùr Glacier is frequented by hikers, and is a route suggested by Parks Canada, which they describe as "*one of the most popular hikes for wilderness enthusiasts*" (https://www.pc.gc.ca/en/pn-np/yt/kluane/activ/randonnee-hiking/dan-zhur). Their suggested hiking route is a 110 km, 8 to 10-day hike that begins where the Duke River crosses the Alaska Highway, and then travels over the Hoge Pass and down Hoge Creek, where it meets the Dań Zhùr Chù'. From here, it leads upriver until it passes the front of the glacier. From the bottom of Hoge Creek, until past the terminus of the glacier, there is a risk of flooding during a rapid drainage from the Dań Zhùr Lake (Figure 5.8). This hike is described by Parks Canada as a route, not a trail, meaning that there is no signage or maintenance, and it is up to the hiker to choose their own route and camping spots. However, there is a description of a suggested route on the webpage, which recommends hiking in the valley bottom, alongside the river, if possible. On July 15th, 2019, just a day after the lake had finished draining, there was a hiker that came across some evidence of the drainage between Hoge Creek and the terminus of the glacier. The hiker, Haley Digel, captured an image of large amounts of wet mud deposited in the trees with some small streams of water running through the vegetation (Figure 5.9), which was published in an article by CBC (Canadian Broadcasting Corporation; https://www.cbc.ca/news/canada/north/glacial-lake-bursts-in-yukon-1.5312116). This mud was likely left behind from flooding in the forest a few days prior as a result of the lake drainage.

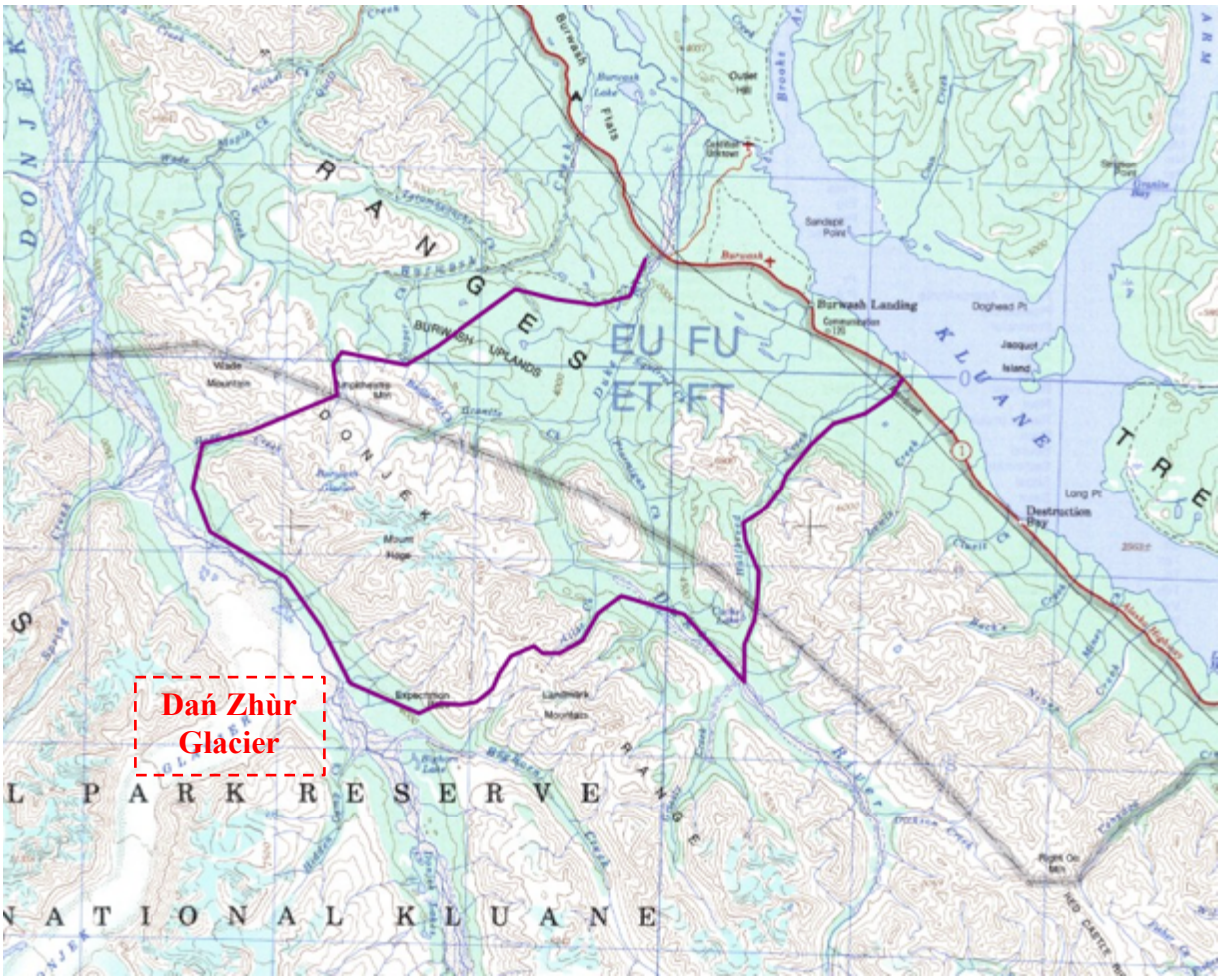

Figure 5.8. Map of Dań Zhùr hiking route, passing the terminus of Dań Zhùr Glacier. Image sourced from Alpine Club of Canada (https://www.alpineclubofcanada.ca/web/ACCMember/Adventures/Summer/2019/Donjek_Glacier_Route_Summer2019.aspx).

Figure 5.9. Photo taken on July 15, 2019, showing the aftermath of the flood in a location ~6.5 km downstream of the terminus of of Dań Zhùr Glacier. Image courtesy of Haley Digel, who was hiking the Dań Zhùr Route during the 2019 drainage event. Image location shown in Figure 5.10.

Another way to see this area is to hike to an area near the Dań Zhùr Glacier and pack raft past the terminus and down the Dań Zhùr Chù'. This is not a route suggested by Parks Canada but could be useful for them to monitor and provide public warnings about, as pack rafters are at a higher risk if they are on the river or near the glacier when an outburst flood occurs.

During the 2019 drainage event, which was the largest since the 1930s (Kochtitzky et al., 2020), there was a visible increase in the extent of water in the Dań Zhùr Chù'. There is no river gauging data available in the study area, but Figure 5.10 marks three locations where Planet satellite imagery enables an assessment of changes in the Dań Zhùr Chù' before, during and after the 2019 drainage event. Downstream from the glacier terminus there was a noticeable change in water extent across the river channel on July 14th, 2019 (see Figure 5.11b), as the drainage was occurring. Figure 5.12 shows a pinch point in the river, about 7 km downstream from the terminus. This is where Hoge Creek enters the Dań Zhùr Chù', where the hiking route suggested by Parks Canada passes. The volume of water flowing through the Dań Zhùr Chù' increased on

July 14th (Figure 5.12b), as the river became less braided and many of the intervening gravel bars disappeared. In these parts of the river there is no permanent infrastructure, so flooding there does not pose any risk to buildings or bridges. However, due to recreational users in the area, this would be a good area to monitor during future drainage events, as there is a higher risk with more recreational traffic.

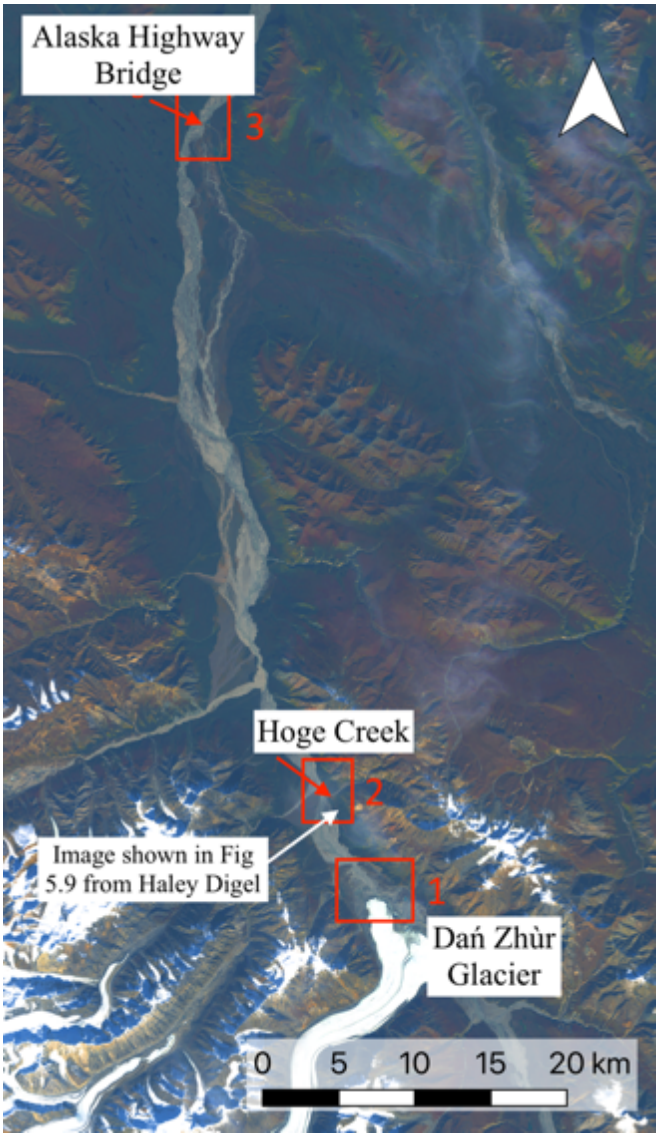

Figure 5.10. Map of the Dań Zhùr Chù' from the Dań Zhùr Glacier to the Alaska Highway bridge; 1) Upper Dań Zhùr Chù' at the toe of the Dań Zhùr Glacier (see Figure 9); 2) Upper Dań Zhùr Chù' at Hoge Creek (see Figure 5.12); and 3) Lower Dań Zhùr Chù' at the Alaska Highway Bridge (see Figure 5.13). Background image is Landsat 8 image from September 6th, 2019, sourced from the USGS Earth Explorer.

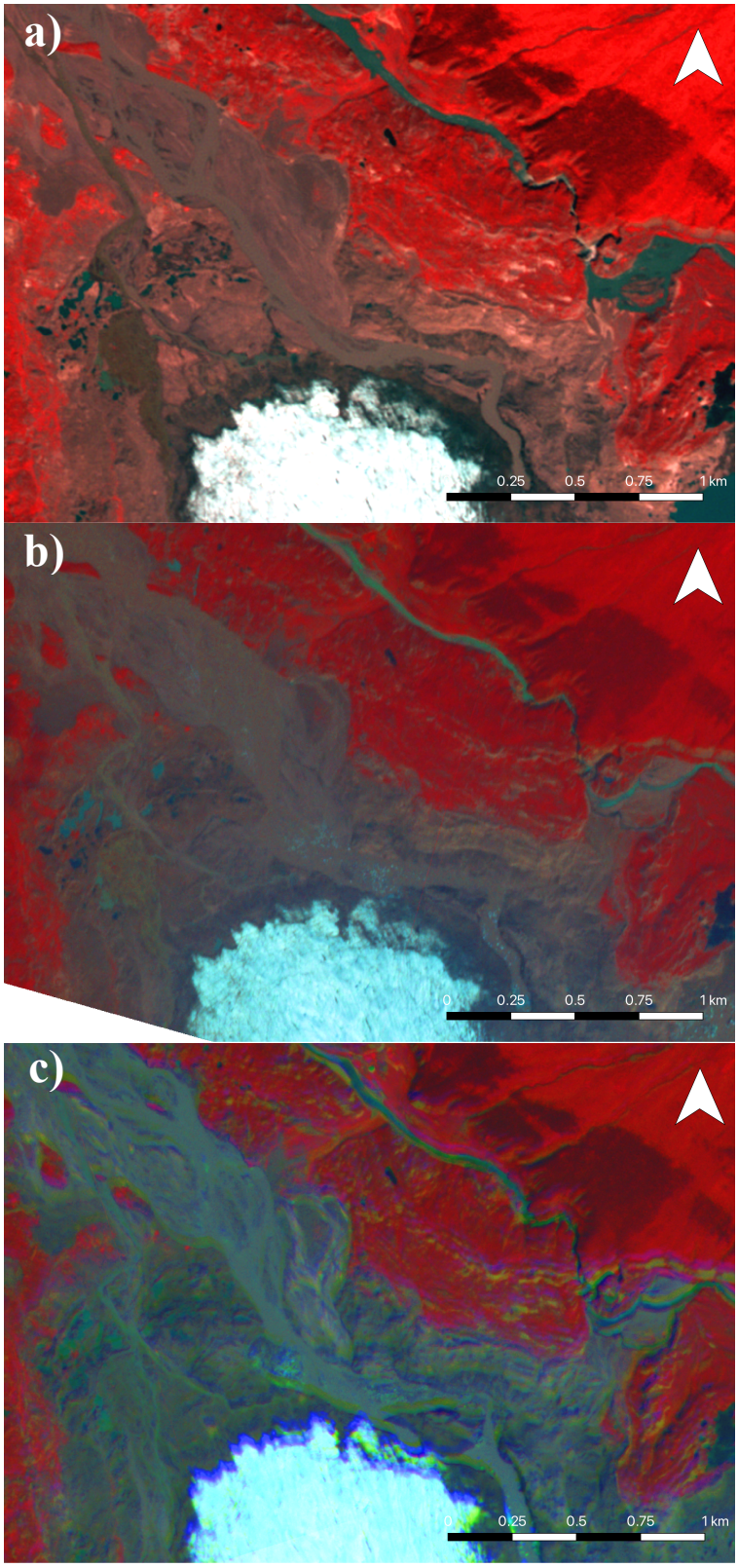

Figure 5.11. Upper Dań Zhùr Chù' at the Dań Zhùr Glacier from a) July 6th, 2019; b) July 14th, 2019; and c) July 27th, 2019 (All images are Planet).

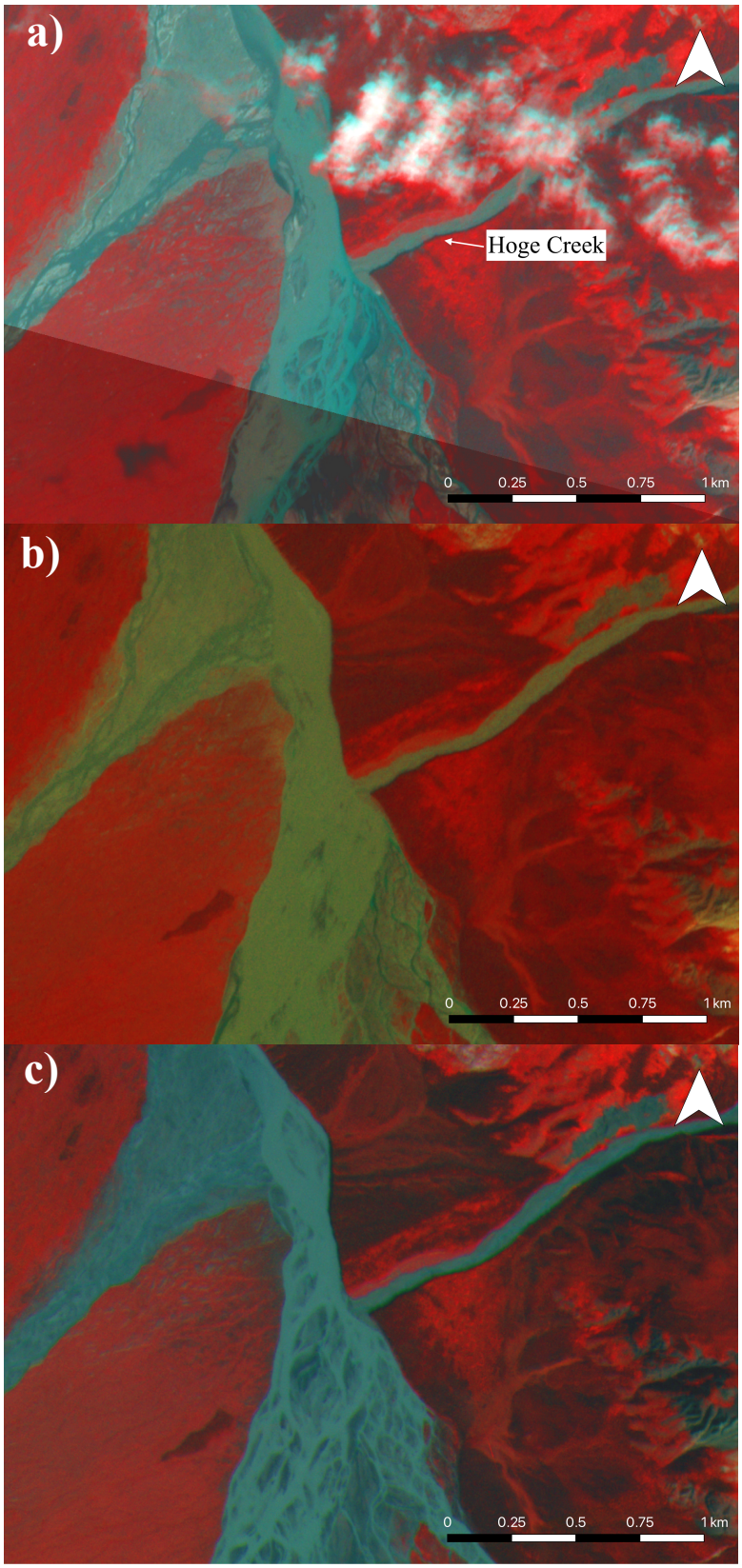

Figure 5.12. Upper Dań Zhùr Chù' at Hoge Creek from a) July 5th, 2019; b) July 14th, 2019; and c) July 27th, 2019 (All images are Planet). Hiking trail is along the north bank of Hoge Creek.

The final area of interest is at the Alaska Highway Bridge, about 50 km downstream of the glacier (Figure 5.13). The bridge was most recently replaced in 2007, and was designed to meet the seismic requirements of the Canadian Highway Bridge Design Code (https://www.whitehorsestar.com/News/theres-a-new-bridge-on-the-block). It is about 270 m long and is made up of 8 spans and is intended to last 75 years. This is the only area along the Dań Zhùr Chù' with current infrastructure that would be affected if a damaging flood occurred. This bridge is part of the primary access route between the US and Yukon, and sees a lot of local, tourist and commercial travel, especially during the summer months, which is when GLOFs generally occur. In Figure 5.13b we can see that there was not a significant increase in water extent on July 14th, 2019, which suggests that there was not a significant risk to the bridge from the 2019 lake drainage, even though it was the largest on record.

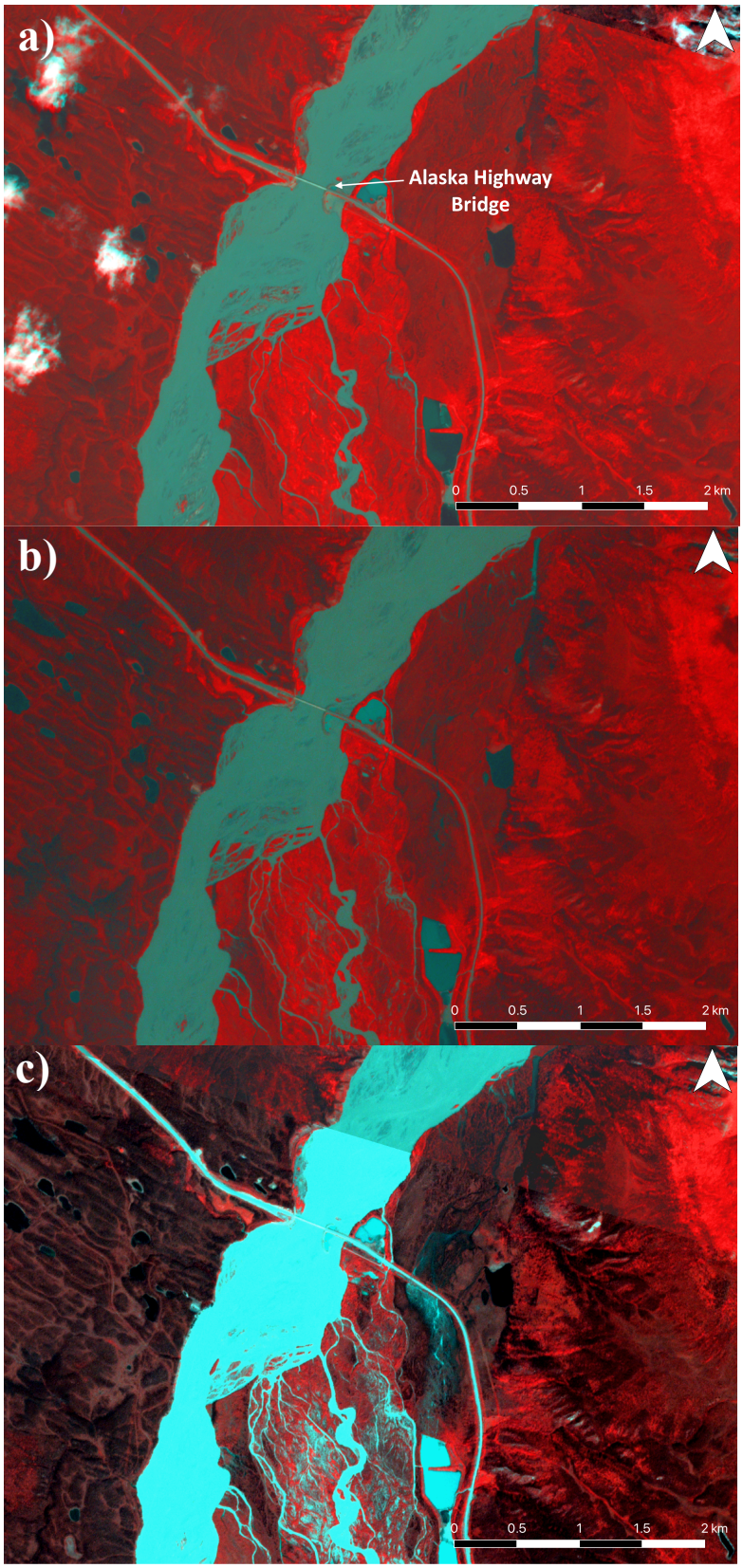

Figure 5.13. Lower Daǹ Zhùr Chù' at the Alaska Highway Bridge from a) July 6th, 2019; b) July 14th, 2019; and c) July 27th, 2019 (All images are Planet).

Before the next surge of Dań Zhùr Glacier, which can be expected to begin around 2024, there is very little to no risk of a GLOF as it is highly unlikely that the lake will form again due to the size of the 2019 ice canyon and its increase in size since then. After the next surge event, the risk of a GLOF is higher as an ice-dammed lake is likely to form again once the advancing terminus creates a partial blockage of the valley and Dań Zhùr Chù'. During the following quiescent phase, it is possible that we will see larger lakes than we did in 2017, 2018 and 2019, due to the increasing size of the basin at the terminus of the glacier as the ice continues to recede.

In the long term it is likely that the risk of GLOFs at Dań Zhùr Glacier will decrease, and maybe even disappear, as the glacier continues to recede, and every surge event reaches a less advanced extent than the previous one. Eventually one of these surge events will not extend far enough into the valley to dam the Dań Zhùr Chù', and no ice-dammed lake will form. It is not possible to provide an accurate prediction for this date, but it will likely be a few decades from now. In combination with glacier recession, the terminus will also thin. A thinner terminus means that the lake would not have to reach the same depth to float the ice. It is possible that the lakes will begin to drain much earlier after the end of a surge, and therefore will never reach the same extent as the lakes we have seen in 2017, 2018 and 2019.

6.0 Conclusions

The main objectives of this study were to describe and explain the patterns and mechanisms of the drainages of Dań Zhùr Lake during the last three surge and quiescent phases, since 1988, as well as the potential current and future downstream risks of any outburst events from Dań Zhùr Lake. To assess any patterns in timing of drainage events over the past three surge cycles, satellite imagery was gathered for the time before and after each event. All three quiescent phases experienced 3-4 drainage events, although the lakes that formed between 1988 and 2019 do not show a clear pattern in drainage timing. There was, however, a pattern between the mechanisms of each drainage. All the rapid drainage events occurred subglacially, but after the final drainage of each surge cycle (the third or fourth drainage) the subglacial channel collapsed to form an ice canyon, while during the first two or three drainage events the roof of the channel remained intact. Dań Zhùr Lake also drains gradually through a subaerial pathway through the Neoglacial maximum moraine to the NE of the glacier terminus when lake levels are very high, but no catastrophic drainage occurs through this pathway as it is approximately 50 m higher than the lakebed.

The 2019 drainage event was the largest over the study period, and air photo derived DEMs obtained when the lake was close to its maximum extent were used to assess the likelihood of flotation of the terminus as a mechanism of drainage. The area where the lake drained in 2019 was found to be very likely to float, as the depth of the lake was over 91.7% of the thickness of the ice at that spot. The change in drainage location between 2019 and 2017/2018 is likely due to the 2019 location being one of the thinnest areas of the terminus, and therefore being the easiest flow route for water to reach the Dań Zhùr Chù' downstream. The size of Dań Zhùr Lake is expected to increase during the next quiescent phase, as the continued glacier recession will expose a larger basin for the lake, and in this case, flotation will continue to be a likely mechanism for drainage. The thinning of the terminus in the future will also possibly lead to drainage events happening sooner after a surge, because if the ice is thinner the lake will not need to reach the same depth as it has done in previous years to cause flotation..

The mechanism of flotation leading to glacial lake drainage is not a new one. Carrivick et al. (2017) determined that the mechanism of drainage for two outburst floods at Russell Glacier in West Greenland, in 2010 and 2012, was very likely flotation. The lake level at the time that drainage began was lower in 2012 than in 2010, which was due to the thinning of the ice at the

terminus of the glacier, which is what we expect to see at Dań Zhùr Glacier in the future. A similar mechanism was observed in East Greenland, at Catalina Lake, which is dammed by the Edward Bailey Glacier (Grinsted et al., 2017). Flotation of the ice shelf begins, and then water flowing beneath the glacier begins to melt it from below, leading to a drainage of the lake beneath the glacier (Grinsted et al., 2017).

The floods caused by drainage events from Dań Zhùr Lake have the potential to be a risk to people and infrastructure downstream. The area close to the glacier is frequented by hikers and pack rafters who could be on or nearby the Dań Zhùr Chù' at the time of a drainage event. Satellite imagery was assessed for downstream changes during the July 2019 drainage event, and there were some noticeable changes in water extent across the river in areas where hikers may be. Photos from a hiker that was in the area around the time of the drainage event of 2019 show large amounts of wet mud deposited in the trees, suggesting that water had been flowing through this area not long before the image was captured.

Over the next surge and quiescent phase, it would be beneficial to monitor the size of the ice dammed lake and thickness of the glacier terminus, to enable determination of when flotation might happen, and subsequently a rapid drainage event. Regular monitoring of satellite imagery should also occur to enable detection of the next surge of Dań Zhùr Glacier. Having this information would diminish the risk to recreational users in downstream areas of the Dań Zhùr Chù'.

7.0 References

Abe, T., Furuya, M., & Sakakibara, D. (2016). Brief communication: twelve-year cyclic surging episodes at Donjek Glacier in Yukon, Canada. *The Cryosphere*, *10*(4), 1427-1432.

Agisoft, L. L. C. (2020). Agisoft metashape user manual, Professional edition, Version 1.6. *Agisoft LLC, St. Petersburg, Russia, from https://www.agisoft.com/pdf/metashape-pro_1_6_en.pdf,* accessed March 11, 2020.

Allen, S. K., Rastner, P., Arora, M., Huggel, C., & Stoffel, M. (2016). Lake outburst and debris flow disaster at Kedarnath, June 2013: hydrometeorological triggering and topographic predisposition. *Landslides*, *13*(6), 1479-1491.

Bazai, N. A., Cui, P., Carling, P. A., Wang, H., Hassan, J., Liu, D., ... & Wen, J. (2020). Increasing glacial lake outburst flood hazard in response to surge glaciers in the Karakoram. *Earth Science Reviews*, 103432.

Bigelow, D. G., Flowers, G. E., Schoof, C. G., Mingo, L. D., Young, E. M., & Connal, B. G. (2020). The role of englacial hydrology in the filling and drainage of an ice-dammed lake, Kaskawulsh Glacier, Yukon, Canada. *Journal of Geophysical Research: Earth Surface*, *125*(2), e2019JF005110.

Björnsson, H. (1974). *Explanations of jökulhlaups from Grímsvötn, Vatnajökull, Iceland*.

Björnsson, H. (1992). Jökulhlaups in Iceland: prediction, characteristics and simulation. *Annals of Glaciology*, *16*, 95-106.

Björnsson, H. (2009). Jokulhlaups in Iceland: sources, release and drainage. *Megaflooding on Earth and Mars. Cambridge University Press, Cambridge*, 50-64.

Carrivick, J. L., & Tweed, F. S. (2016). A global assessment of the societal impacts of glacier outburst floods. *Global and Planetary Change*, *144*, 1-16.

Carrivick, J. L., Tweed, F. S., Ng, F., Quincey, D. J., Mallalieu, J., Ingeman-Nielsen, T., ... & Russell, A. J. (2017). Ice-dammed lake drainage evolution at Russell Glacier, West Greenland. *Frontiers in Earth Science*, *5*, 100.

Chen, Y., Xu, C., Chen, Y., Li, W., & Liu, J. (2010). Response of glacial-lake outburst floods to climate change in the Yarkant River basin on northern slope of Karakoram Mountains, China. *Quaternary International*, *226*(1-2), 75-81.

Clague, J. J., & Evans, S. G. (2000). A review of catastrophic drainage of moraine-dammed lakes in British Columbia. *Quaternary Science Reviews*, *19*(17-18), 1763-1783.

Clague, J. J., & O'Connor, J. E. (2015). Glacier-related outburst floods. In *Snow and ice-related hazards, risks and disasters* (pp. 487-519). Academic Press.

Clarke, G. K., Schmok, J. P., Ommanney, C. S. L., & Collins, S. G. (1986). Characteristics of surge-type glaciers. *Journal of Geophysical Research: Solid Earth*, *91*(B7), 7165-7180.

Clarke, G. K. C., & Mathews, W. H. (1981). Estimates of the magnitude of glacier outburst floods from Lake Donjek, Yukon Territory, Canada. *Canadian Journal of Earth Sciences*, *18*(9), 1452-1463.

Cruikshank, J. (2005). *Do glaciers listen?: local knowledge, colonial encounters, and social imagination*. UBC Press.

Denton, G. H., & Stuiver, M. (1966). Neoglacial chronology, northeastern Saint Elias Mountains, Canada. *American Journal of Science*, *264*(8), 577-599.

Dussaillant, A., Benito, G., Buytaert, W., Carling, P., Meier, C., & Espinoza, F. (2010). Repeated glacial-lake outburst floods in Patagonia: an increasing hazard?. *Natural hazards*, *54*(2), 469-481.

Geertsema, M., & Clague, J. J. (2005). Jökulhlaups at Tulsequah Glacier, northwestern British Columbia, Canada. *The Holocene*, *15*(2), 310-316.

Glen, J. W. (1954). The stability of ice-dammed lakes and other water-filled holes in glaciers. *Journal of Glaciology*, *2*(15), 316-318.

Grinsted, A., Hvidberg, C. S., Campos, N., & Dahl-Jensen, D. (2017). Periodic outburst floods from an ice-dammed lake in East Greenland. *Scientific Reports*, *7*(1), 1-6.

Haeberli, W., Whiteman, C. A., & Shroder, J. F. (Eds.). (2015). *Snow and ice-related hazards, risks, and disasters*. Waltham, MA: Academic Press.

Harrison, W. D., Osipova, G. B., Nosenko, G. A., Espizua, L., Kääb, A., Fischer, L., ... & Lai, A. W. (2015). Glacier surges. In *Snow and ice-related hazards, risks and disasters* (pp. 437-485). Academic Press.

Harrison, S., Kargel, J. S., Huggel, C., Reynolds, J., Shugar, D. H., Betts, R. A., ... & Schaub, Y. (2018). Climate change and the global pattern of moraine-dammed glacial lake outburst floods. *The Cryosphere*, *12*.

Higgins, A. K. (1970). On some ice-dammed lakes in the Frederikshåb district, south-west Greenland. *Meddelelser Fra Dansk Geologisk Forening*, *19*, 378-97.

Hock, R., G. Rasul, C. Adler, B. Cáceres, S. Gruber, Y. Hirabayashi, M. Jackson, A. Kääb, S. Kang, S. Kutuzov, A. Milner, U. Molau, S. Morin, B. Orlove, and H. Steltzer, 2019: High Mountain Areas. In*: IPCC Special Report on the Ocean and Cryosphere in a Changing Climate* [H.-O. Pörtner, D.C. Roberts, V. Masson-Delmotte, P. Zhai, M. Tignor, E. Poloczanska, K. Mintenbeck, A. Alegría, M. Nicolai, A. Okem, J. Petzold, B. Rama, N.M. Weyer (eds.)].

Iturrizaga, L. (2011). Glacier lake outburst floods. *Encyclopedia of Snow, Ice and Glaciers*, 381-399.

Jóhannesson, T. (2002). The initiation of the 1996 jökulhlaup from Lake Grímsvötn, Vatnajökull, Iceland. *IAHS Publication*, *271*, 57-64.

Knight, P. G., & Russell, A. J. (1993). Most recent observations of the drainage of an ice-dammed lake at Russell Glacier, West Greenland, and a new hypothesis regarding mechanisms of drainage initiation. *Journal of Glaciology*, *39*(133), 701-703.

Kochtitzky, W., Copland, L., Painter, M. and Dow, C. In review. Draining and filling of ice dammed lakes at the terminus of surge-type Dań Zhùr (Donjek Glacier), Yukon, Canada. *Canadian Journal of Earth Sciences*.

Kochtitzky, W., Jiskoot, H., Copland, L., Enderlin, E., Mcnabb, R., Kreutz, K., & Main, B. (2019). Terminus advance, kinematics and mass redistribution during eight surges of Donjek Glacier, St. Elias Range, Canada, 1935 to 2016. *Journal of Glaciology*, 1-15.

Maag, H., & Müller, F. (1972). Ice-dammed lakes on Axel Heiberg Island, with special reference to the geomorphological effect of the outflowing lake water. *International Geographical Union*.

McKnight, E. A., Swanson, H., Brahney, J., & Hik, D. S. (2021). The physical and chemical limnology of Yukon's largest lake, Lhù'ààn Mân'(Kluane Lake), prior to the 2016 'A'äy Chù' diversion. *Arctic Science*, 1-24.

Meier, M. F., & Post, A. (1969). What are glacier surges? *Canadian Journal of Earth Sciences*, *6*(4), 807-817.

Mergili, M., Pudasaini, S. P., Emmer, A., Fischer, J. T., Cochachin, A., & Frey, H. (2020). Reconstruction of the 1941 GLOF process chain at Lake Palcacocha (Cordillera Blanca, Peru). *Hydrology and Earth System Sciences*, *24*(1), 93-114.

Perchanok, M. S. (1980). *History of a glacier-dammed lake on Donjek River, Yukon; by Max S. Perchanok* (Doctoral dissertation, Carleton University).

Round, V., Leinss, S., Huss, M., Haemmig, C., & Hajnsek, I. (2017). Surge dynamics and lake outbursts of Kyagar Glacier, Karakoram. *The Cryosphere*, *11*(2), 723-739.

Russell, A. J., Carrivick, J. L., Ingeman-Nielsen, T2., Yde, J. C., & Williams, M. (2011). A new cycle of jökulhlaups at Russell Glacier, Kangerlussuaq, West Greenland. *Journal of Glaciology*, *57*(202), 238-246.

Sevestre, H., & Benn, D. I. (2015). Climatic and geometric controls on the global distribution of surge-type glaciers: implications for a unifying model of surging. *Journal of Glaciology*, *61*(228), 646-662.

Shean, D. E., O. Alexandrov, Z. Moratto, B. E. Smith, I. R. Joughin, C. C. Porter, Morin, P. J. (2016) An automated, open-source pipeline for mass production of digital elevation models (DEMs) from very high-resolution commercial stereo satellite imagery. *ISPRS J. Photogramm. Remote Sens, 116*, 101-117.

Shugar, D. H., Clague, J. J., Best, J. L., Schoof, C., Willis, M. J., Copland, L., & Roe, G. H. (2017). River piracy and drainage basin reorganization led by climate-driven glacier retreat. *Nature Geoscience*, *10*(5), 370-375.

Shugar, D. H., Burr, A., Haritashya, U. K., Kargel, J. S., Watson, C. S., Kennedy, M. C., ... & Strattman, K. (2020). Rapid worldwide growth of glacial lakes since 1990. *Nature Climate Change*, *10*(10), 939-945.

Shumskiy, P. A. (1960). Density of glacier ice. *Journal of Glaciology*, *3*(27), 568-573.

Somos-Valenzuela, M. A., Chisolm, R. E., Rivas, D. S., Portocarrero, C., & McKinney, D. C. (2016). Modeling a glacial lake outburst flood process chain: the case of Lake Palcacocha and Huaraz, Peru. *Hydrology and Earth System Sciences*, *20*(6), 2519.

Thomson, L., & Copland, L. (2016). White Glacier 2014, Axel Heiberg Island, Nunavut: mapped using structure from motion methods. *Journal of Maps*, *12*(5), 1063-1071.

Tómasson, H. (1996). The jökulhlaup from Katla in 1918. *Annals of Glaciology*, *22*, 249-254.

Walder, J. S., & Costa, J. E. (1996). Outburst floods from glacier-dammed lakes: The effect of mode of lake drainage on flood magnitude. *Earth Surface Processes and Landforms*, *21*(8), 701-723.

Wolfe, D. F., Kargel, J. S., & Leonard, G. J. (2014). Glacier-dammed ice-marginal lakes of Alaska. In *Global Land Ice Measurements from Space* (pp. 263-295). Springer, Berlin, Heidelberg.

Yamada, T., & Sharma, C. K. (1993). Glacier lakes and outburst floods in the Nepal Himalaya. *IAHS Publications-Publications of the International Association of Hydrological Sciences*, *218*, 319-330.

Young, E. M., Flowers, G. E., Berthier, E., & Latto, R. (2021). An imbalancing act: the delayed dynamic response of the Kaskawulsh Glacier to sustained mass loss. *Journal of Glaciology*, *67*(262), 313-330.